CHAPTER THREE

The Per-Unit-Length Parameters

The per-unit-length parameter matrices of inductance, **L**, capacitance, **C**, resistance, **R**, and conductance, **G**, are essential ingredients in the determination of the MTL voltages and currents from the MTL equations. It is important to recall that, under the fundamental TEM field structure assumption, *the per-unit-length parameters of inductance, capacitance, and conductance are determined as a static (dc) solution to Laplace's equation, e.g.,* $\nabla^2\phi(x, y) = 0$, *in the two-dimensional cross-sectional* (x, y) *plane of the line.* Therefore the entries in **L**, **C**, and **G** are governed by the fields external to the line conductors and are determined as *static field solutions in the transverse plane for perfect conductors.* The entries in the per-unit-length resistance matrix, **R**, are governed by the fields interior to the conductors for imperfect conductors. In the case of perfect line conductors, $\mathbf{R} = \mathbf{0}$. Technically, the fields exterior and interior to imperfect conductors interact so that the entries in **R** cannot be independently determined as the resistances of the isolated conductors. For typical line dimensions and frequencies of excitation the entries in **R** can be determined as the resistances of the isolated conductors to a reasonable degree of approximation. Cases where this interaction cannot be ignored will be discussed as needed.

The purpose of this chapter is to investigate methods, analytical and numerical, for determining these per-unit-length parameters. The ease with which we can determine these for a particular MTL cross-sectional structure depends on the properties of the MTL. For example, we will find that for wire conductors (circular cylindrical cross sections) that are relatively widely spaced and immersed in a homogeneous surrounding medium, some simple, closed-form analytical expressions can be obtained for the per-unit-length parameters. If the wires are closely spaced and/or the medium is inhomogeneous, one must typically resort to approximate numerical methods to obtain the per-unit-length parameters. Conductors of rectangular cross section such as are found on printed circuit boards (PCBs) also typically require approximate numerical methods for their determination regardless of whether the medium is

homogeneous or inhomogeneous (as is typically the case with PCB's). There exist some analytical solutions for the per-unit-length parameters for a two-conductor line having conductors of rectangular cross section but these are often quite involved. These analytical solution techniques generally attempt to transform the desired problem to a simpler problem using a transformation of coordinate variables, e.g., the Schwarz–Christoffel transformation. It is important to keep in mind that efficiency of solution of this step is critically determined by the class of MTL being considered.

3.1 DEFINITIONS OF THE PER-UNIT-LENGTH PARAMETER MATRICES L, C, G

We first review the fundamental definitions, obtained in the previous chapter, of the per-unit-length parameter matrices of inductance, **L**, capacitance, **C**, and conductance, **G**. Recall that these per-unit-length parameters are determined as *static field solutions in the transverse plane for perfect line conductors.* There are numerous methods, analytic and numerical, for this static two-dimensional problem. The entries in the per-unit-length resistance matrix, **R**, will be obtained in Section 3.6. Again we will restrict our discussions to *uniform lines.*

3.1.1 The Per-Unit-Length Inductance Matrix, L

The entries in the per-unit-length inductance matrix, **L**, relate *the total magnetic flux penetrating the i-th circuit, per unit of line length, to all the line currents producing it as*

$$\Psi = \mathbf{L}\mathbf{I} \tag{3.1a}$$

or, in expanded form,

$$\begin{bmatrix} \psi_1 \\ \psi_2 \\ \vdots \\ \psi_n \end{bmatrix} = \begin{bmatrix} l_{11} & l_{12} & \cdots & l_{1n} \\ l_{12} & l_{22} & \cdots & l_{2n} \\ \vdots & \vdots & \ddots & \vdots \\ l_{1n} & l_{2n} & \cdots & l_{nn} \end{bmatrix} \begin{bmatrix} I_1 \\ I_2 \\ \vdots \\ I_n \end{bmatrix} \tag{3.1b}$$

If we interpret the above relations in a manner similar to the n-port parameters [A.2], we obtain the following relations for the entries in **L**:

$$l_{ii} = \left.\frac{\psi_i}{I_i}\right|_{I_1 = \cdots = I_{i-1} = I_{i+1} = \cdots = I_n = 0} \tag{3.2a}$$

$$l_{ij} = \left.\frac{\psi_i}{I_j}\right|_{I_1 = \cdots = I_{j-1} = I_{j+1} = \cdots = I_n = 0} \tag{3.2b}$$

Thus we can compute these inductances by placing a current on one conductor

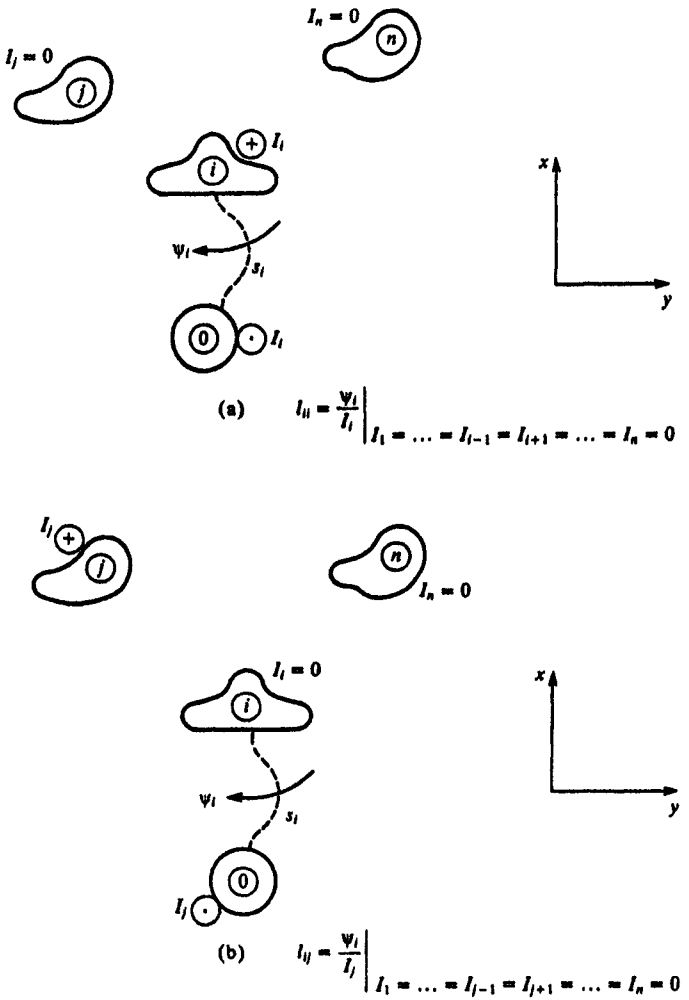

FIGURE 3.1 Illustration of the definitions of flux through a circuit for determination of the per-unit-length inductances: (a) self-inductances, l_{ii}, and (b) mutual inductances, l_{ij}.

(and returning it on the reference conductor), setting the currents on all other conductors to zero and determining the magnetic flux, per unit of line length, penetrating the other *circuit*. The definition of the *i-th circuit* is critically important to obtaining the correct value and sign of these elements. This important concept is illustrated in Fig. 3.1. The *i-th circuit* is the surface between the reference conductor and the *i*-th conductor (which is of arbitrary shape but is uniform along the line). This surface shape may be a flat surface or some other shape so long as this shape is uniform along the line. The magnetic flux per-unit-length penetrating this surface (circuit) is *defined* as being in the

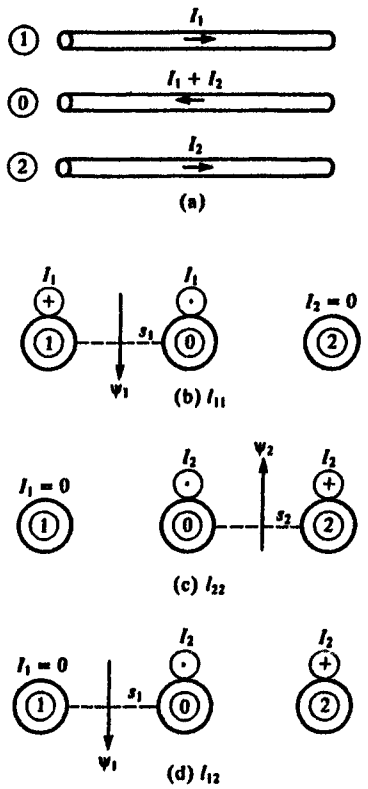

FIGURE 3.2 Illustrations of the derivation of the per-unit-length inductances for a ribbon cable structure.

clockwise direction around the i-th conductor when looking in the direction of increasing z. In other words, *the flux direction, ψ_i, through surface s_i is the direction magnetic flux would be generated by the current of the i-th conductor.* Figure 3.1(a) shows the calculation of l_{ii}, and Fig. 3.1(b) shows the calculation of l_{ij}.

In order to illustrate this important concept further, consider a three-conductor line consisting of three wires lying in a plane where the middle wire is chosen, arbitrarily, as the reference conductor as shown in Fig. 3.2(a). The surfaces and individual configurations for computing l_{11}, l_{22}, and l_{12} are shown in the remaining figures. Observe that the surface for ψ_2 is between conductor number 2 and the reference conductor but observe the desired direction of this flux; it is chosen with respect to the magnetic flux that would be produced by current I_2 on conductor number 2. So, *the flux direction for the i-th circuit is defined by the direction of the current on the i-th conductor and the right-hand rule when looking in the direction of increasing z.*

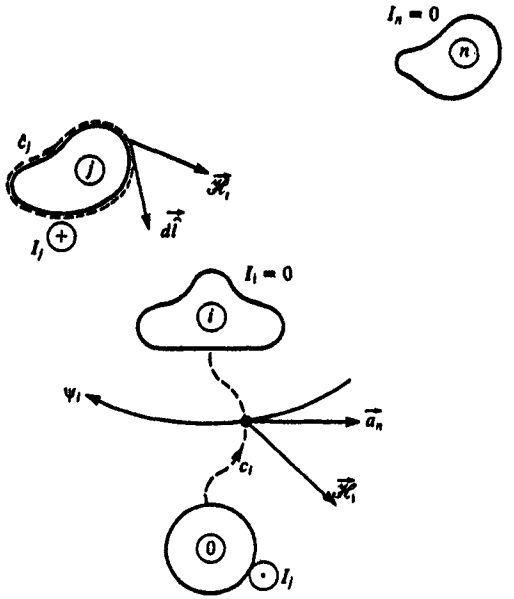

FIGURE 3.3 Illustration of the contours and flux directions for the general derivation of the per-unit-length inductances.

This computation requires that the magnetic flux penetrating the surface by the desired current (and having the current return on the reference conductor) be computed. There are many ways of accomplishing this task. In some cases an analytical solution (exact or approximate) can be obtained, whereas in other cases numerical approximation techniques must be used. In either case, the precise definition of each of these l_{ij} computations is, from Chapter 1,

$$l_{ij} = \left.\frac{\psi_i}{I_j}\right|_{I_1 = \cdots = I_{j-1} = I_{j+1} = \cdots = I_n = 0} = \frac{-\mu \displaystyle\int_{c_i} \vec{\mathcal{H}}_i \cdot \vec{a}_n \, dl}{\displaystyle\oint_{c_j} \vec{\mathcal{H}}_i \cdot d\vec{l}} \tag{3.3}$$

which is illustrated in Fig. 3.3.

Although the above method is valid regardless of whether the medium is homogeneous or inhomogeneous in μ, if the medium is *homogeneous* in μ (as are typical dielectric media), then **L** can be obtained from **C** using the fundamental relationship derived previously

$$\mathbf{L} = \mu\varepsilon\mathbf{C}^{-1} \tag{3.4}$$

3.1.2 The Per-Unit-Length Capacitance Matrix, C

The entries in the per-unit-length capacitance matrix, **C**, relate the *total charge on the i-th conductor per unit of line length to all of the line voltages producing it* as

$$\mathbf{Q} = \mathbf{CV} \tag{3.5a}$$

or, in expanded form,

$$\begin{bmatrix} q_1 \\ q_2 \\ \vdots \\ q_n \end{bmatrix} = \begin{bmatrix} \sum_{k=1}^{n} c_{1k} & -c_{12} & \cdots & -c_{1n} \\ -c_{12} & \sum_{k=1}^{n} c_{2k} & \cdots & -c_{2n} \\ \vdots & \vdots & \ddots & \vdots \\ -c_{1n} & -c_{2n} & \cdots & \sum_{k=1}^{n} c_{nk} \end{bmatrix} \begin{bmatrix} V_1 \\ V_2 \\ \vdots \\ V_n \end{bmatrix} \tag{3.5b}$$

If we denote the entries in **C** as $[\mathbf{C}]_{ij}$, these can be obtained by interpreting (3.5) as an n-port relation and applying the usual constraints of setting all voltages except the j-th voltage, V_j, to zero and determining the charge, q_i, on the i-th conductor (and $-q_i$ on the reference conductor) to give $[\mathbf{C}]_{ij}$. The particular form for the entries in **C** in (3.5b) can be readily seen by placing the per-unit-length capacitances between the conductors and writing the usual node-voltage equations of lumped-circuit theory [A.2].

A simpler form for obtaining the elements of **C** is obtained by inverting (3.5a) as

$$\mathbf{V} = \mathbf{PQ} \tag{3.6a}$$

or, in expanded form,

$$\begin{bmatrix} V_1 \\ V_2 \\ \vdots \\ V_n \end{bmatrix} = \begin{bmatrix} p_{11} & p_{12} & \cdots & p_{1n} \\ p_{12} & p_{22} & \cdots & p_{2n} \\ \vdots & \vdots & \ddots & \vdots \\ p_{1n} & p_{2n} & \cdots & p_{nn} \end{bmatrix} \begin{bmatrix} 1_1 \\ q_2 \\ \vdots \\ q_n \end{bmatrix} \tag{3.6b}$$

where

$$\mathbf{C} = \mathbf{P}^{-1} \tag{3.6c}$$

The entries in **P** are referred to as the *coefficients of potential.* Once the entries in **P** are obtained, **C** is obtained via (3.6c). The coefficients of potential are obtained from (3.6b) as

$$p_{ii} = \left.\frac{V_i}{q_i}\right|_{q_1 = \cdots = q_{i-1} = q_{i+1} = \cdots = q_n = 0} \tag{3.7a}$$

$$p_{ij} = \left.\frac{V_i}{q_j}\right|_{q_1 = \cdots = q_{j-1} = q_{j+1} = \cdots = q_n = 0} \tag{3.7b}$$

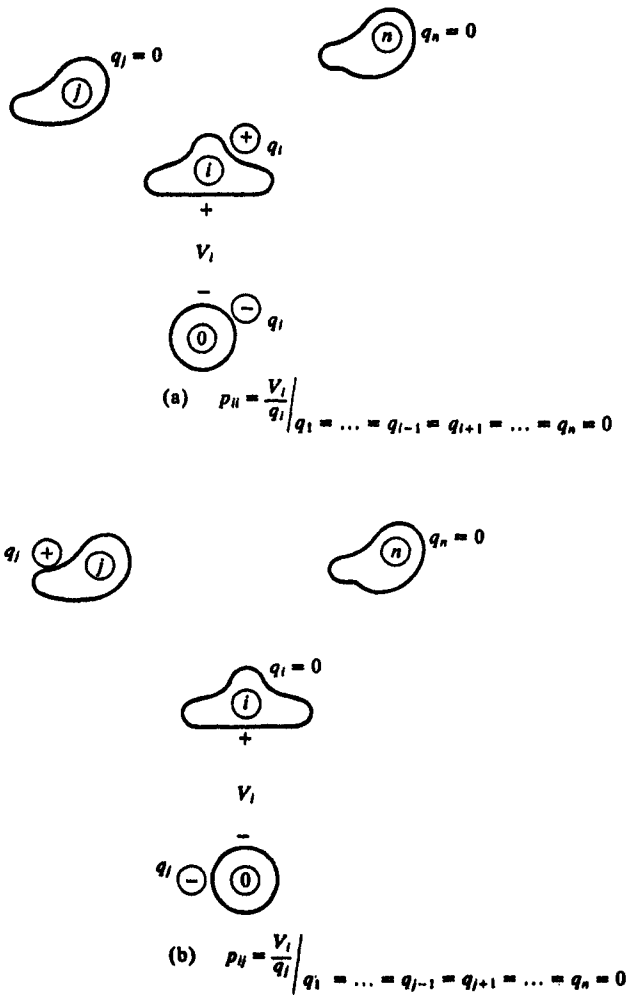

FIGURE 3.4 Illustrations of the determination of the per-unit-length coefficients of potential: (a) self terms, p_{ii}, and (b) mutual terms, p_{ij}.

These relationships show that to determine p_{ij} we place charge q_j on conductor j with no charge on the other conductors (but $-q_j$ on the reference conductor) and determine the resulting voltage V_i on conductor i (between it and the reference conductor with the voltage positive at the i-th conductor). These concepts are illustrated in Fig. 3.4. Once **P** is obtained in this fashion, **C** is obtained as the inverse of **P** as shown in (3.6c). It is important to point out that the self-capacitance between the i-th conductor and the reference conductor, c_{ii}, *is not simply the entry in the i-th row and i-th column of* **C**. Observe the form of the entries in **C** given in (3.5b). The off-diagonal entries are the negatives of

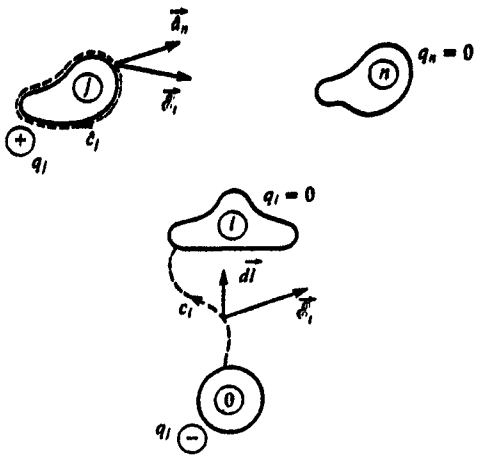

FIGURE 3.5 Illustration of the general definitions of contours for the determination of charge and voltage in the determination of the per-unit-length coefficients of potential.

the mutual capacitances between the pairs of conductors whereas the main-diagonal entries are the sum of the self-capacitance and the mutual capacitances in that row (or column). Therefore, to obtain the self-capacitance, c_{ii}, we *sum the entries in the i-th row (or column) of* **C**.

This is again a static problem in the two-dimensional transverse plane. There are many ways to compute the p_{ij} from the n-port definitions in (3.7). However, the fundamental definition was derived in Chapter 1 and is

$$p_{ij} = \left.\frac{V_i}{q_j}\right|_{q_1 = \cdots = q_{j-1} = q_{j+1} = \cdots q_n = 0} = \frac{-\int_{c_i} \vec{\mathcal{E}}_t \cdot d\vec{l}}{\varepsilon \oint_{c_j} \vec{\mathcal{E}}_t \cdot \vec{a}_n \, dl} \tag{3.8}$$

as illustrated in Fig. 3.5.

This method is valid regardless of whether the surrounding medium is homogeneous or inhomogeneous in ε. If the surrounding medium is *homogeneous* in ε, we can alternatively obtain **C** from **L** using the fundamental relationship

$$\mathbf{C} = \mu\varepsilon\mathbf{L}^{-1} \tag{3.9}$$

3.1.3 The Per-Unit-Length Conductance Matrix, G

The per-unit-length conductance matrix, G, relates the *total transverse conduction current passing between the conductors per unit of line length to all the line voltages producing it* as

$$\mathbf{I}_t = \mathbf{G}\mathbf{V} \tag{3.10a}$$

or, in expanded form,

$$\begin{bmatrix} I_{t1} \\ I_{t2} \\ \vdots \\ I_{tn} \end{bmatrix} = \begin{bmatrix} \sum_{k=1}^{n} g_{1k} & -g_{12} & \cdots & -g_{1n} \\ -g_{12} & \sum_{k=1}^{n} g_{2k} & \cdots & -g_{2n} \\ \vdots & \vdots & \ddots & \vdots \\ -g_{1n} & -g_{2n} & \cdots & \sum_{k=1}^{n} g_{nk} \end{bmatrix} \begin{bmatrix} V_1 \\ V_2 \\ \vdots \\ V_n \end{bmatrix} \tag{3.10b}$$

Again, the particular forms of the entries in G in (3.10b) can be readily seen by placing the per-unit-length conductances between the conductors and writing the usual node-voltage equations of lumped-circuit theory [A.2].

Once again, the entries in G can be determined as several subproblems by interpreting (3.10b) as an *n port*. For example, to determine the entry in G in the i-th row and j-th column (which, according to (3.10b), is *not* g_{ij}) we could enforce a voltage between the j-th conductor and the reference conductor, V_j, with all other conductor voltages set to zero, $V_1 = \cdots = V_{j-1} = V_{j+1} = \cdots = V_n = 0$, and determine the transverse current, I_{ti}, flowing between the i-th conductor and the reference conductor. Denoting each of the entries in G as $[\mathbf{G}]_{ij}$ we have

$$[\mathbf{G}]_{ij} = \left.\frac{I_{ti}}{V_j}\right|_{V_1 = \cdots = V_{j-1} = V_{j+1} = \cdots = V_n = 0} \tag{3.11}$$

$$= \frac{\oint_{\mathcal{C}_i} \vec{\mathscr{H}}_t \cdot \hat{a}_n \, dl}{-\int_{c_j} \vec{\mathscr{E}}_t \cdot d\vec{l}}$$

as illustrated in Fig. 3.6.

Conversely we could invert the relationship in (3.10) as for the case of the capacitance matrix and determine the entries in that matrix. If the medium is *homogeneous* in σ, we can obtain G from either L or C using the fundamental

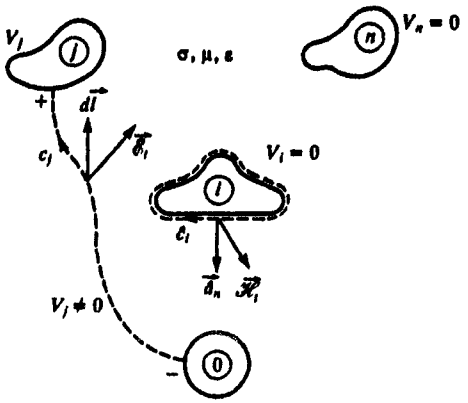

FIGURE 3.6 Contours for the determination of the per-unit-length conductances.

relationships obtained for a *homogeneous medium*:

$$\mathbf{G} = \mu\sigma\mathbf{L}^{-1} \tag{3.12}$$

$$= \frac{\sigma}{\varepsilon}\mathbf{C}$$

This result, although proven in Chapter 2, is apparent since the transverse conduction current density is related to the transverse electric field as $\vec{\mathbf{J}}_t = \sigma\vec{\mathbf{E}}_t$ and the per-unit-length capacitance matrix, C, is governed solely by the transverse electric field. There are two different mechanisms that introduce losses in the medium. The first is through a nonzero conductivity and the other is through polarization loss [A.1]. Both mechanisms are implicitly included in the conductivity parameter. The incorporation of losses in the media for inhomogeneous media will be examined in Section 3.6.1 and is relatively straightforward as a modification of the determination of C for the inhomogeneous medium. If the surrounding medium, homogeneous or inhomogeneous, is lossless, i.e., the conductivities are zero, then $\mathbf{G} = \mathbf{0}$.

3.1.4 The Generalized Capacitance Matrix, $\mathscr{C}$

The above definitions as well as the derivation of the MTL equations assume that we (arbitrarily) select one of the $(n + 1)$ conductors as the *reference conductor* to which all the n voltages, V_i, are referenced. Once the reference conductor is chosen, all the per-unit-length parameter matrices must be computed for that choice consistently. Although the choice of reference conductor is arbitrary, choosing one of the $(n + 1)$ conductors over another as reference may facilitate the computation of the per-unit-length parameters. For

example, if n of the conductors are wires and the remaining conductor is an infinite, perfectly conducting plane, we will show that choice of the plane as the reference conductor simplifies the calculation of the per-unit-length parameters. However, choice of this plane as reference is not mandatory; we could choose instead one of the n wires as reference conductor. In this section we describe a technique for computing a certain per-unit-length parameter matrix, the *generalized capacitance matrix*, $\mathscr{C}$, without regard to choice of reference conductor. Once this is computed, the other per-unit-length parameter matrices. L, C, and G, can be easily computed from it for a particular choice of reference conductor.

The MTL voltages, V_i, are defined to be between each conductor and the reference conductor. We may also define the potentials, ϕ_i, of each of the $(n + 1)$ conductors with respect to some reference point or line that is parallel to the z axis. The total charge per unit of line length, q_i, of each of the $(n + 1)$ conductors can be related to their potentials, ϕ_i, for $i = 0, 1, 2, \ldots, n$ with the $(n + 1) \times (n + 1)$ generalized capacitance matrix, $\mathscr{C}$, as

$$\mathbf{Q}' = \mathscr{C}\Phi \tag{3.13a}$$

or, in expanded form, as

$$\begin{bmatrix} q_0 \\ q_1 \\ \vdots \\ q_n \end{bmatrix} = \begin{bmatrix} \mathscr{C}_{00} & \mathscr{C}_{01} & \cdots & \mathscr{C}_{0n} \\ \mathscr{C}_{10} & \mathscr{C}_{11} & \cdots & \mathscr{C}_{1n} \\ \vdots & \vdots & \ddots & \vdots \\ \mathscr{C}_{n0} & \mathscr{C}_{n1} & \cdots & \mathscr{C}_{nn} \end{bmatrix} \begin{bmatrix} \phi_0 \\ \phi_1 \\ \vdots \\ \phi_n \end{bmatrix} \tag{3.13b}$$

Observe that $\mathscr{C}$ is $(n + 1) \times (n + 1)$ whereas the previous per-unit-length parameter matrices, L, C, and G, are $n \times n$. Also the generalized capacitance matrix, like the transmission-line-capacitance matrix, is symmetric, i.e., $\mathscr{C}_{ij} = \mathscr{C}_{ji}$, for similar reasons. It can be shown that for a charge-neutral system as is the case for the MTL, the reference potential terms for the choice of reference point for these potentials, ϕ_i, vanishes as the reference point recedes to infinity so that the choice of reference point does not affect the determination of the transmission-line-capacitance matrix, C, from the generalized capacitance matrix [B.1, C.5].

Suppose that $\mathscr{C}$ has been computed and we select a reference conductor. Without loss of generality let us select the reference conductor as the zeroth conductor. In order to obtain the $n \times n$ capacitance matrix, C, from $\mathscr{C}$, define the MTL line voltages, *with respect to this zeroth reference conductor*, as

$$V_i = \phi_i - \phi_0 \tag{3.14}$$

for $i = 1, 2, \ldots, n$. We assume that *the entire system of* $(n + 1)$ *conductors is charge neutral*, i.e., $q_0 + q_1 + q_2 + \cdots + q_n = 0$. Therefore the charge (per unit

of line length) on the zeroth conductor can be written in terms of the charges on the other n conductors as

$$q_0 = -\sum_{k=1}^{n} q_k \tag{3.15}$$

Denote the entries in the i-th row and j-th column of the per-unit-length capacitance matrix, *with the zeroth conductor chosen as reference conductor*, as C_{ij}:

$$\begin{bmatrix} q_1 \\ q_2 \\ \vdots \\ q_n \end{bmatrix} = \begin{bmatrix} C_{11} & C_{12} & \cdots & C_{1n} \\ C_{12} & C_{22} & \cdots & C_{2n} \\ \vdots & \vdots & \ddots & \vdots \\ C_{1n} & C_{2n} & \cdots & C_{nn} \end{bmatrix} \begin{bmatrix} V_1 \\ V_2 \\ \vdots \\ V_n \end{bmatrix} \tag{3.16}$$

Comparing (3.16) to (3.5b) we observe that $C_{ii} = \sum_{k=1}^{n} c_{ik}$ and $C_{ij} = -c_{ij}$. Substituting (3.14) and (3.15) into (3.13) and expanding gives

$$\left.\begin{aligned} -\sum_{k=1}^{n} q_k &= \mathscr{C}_{01}V_1 + \mathscr{C}_{02}V_2 + \cdots + \mathscr{C}_{0n}V_n + \left(\sum_{m=0}^{n} \mathscr{C}_{0m}\right)\phi_0 \\ q_1 &= \mathscr{C}_{11}V_1 + \mathscr{C}_{12}V_2 + \cdots + \mathscr{C}_{1n}V_n + \left(\sum_{m=0}^{n} \mathscr{C}_{1m}\right)\phi_0 \\ &\vdots \\ q_n &= \mathscr{C}_{n1}V_1 + \mathscr{C}_{n2}V_2 + \cdots + \mathscr{C}_{nn}V_n + \left(\sum_{m=0}^{n} \mathscr{C}_{nm}\right)\phi_0 \end{aligned}\right\} \tag{3.17}$$

Adding all equations in (3.17) gives

$$\begin{aligned} 0 = &\left(\sum_{m=0}^{n} \mathscr{C}_{m1}\right)V_1 + \left(\sum_{m=0}^{n} \mathscr{C}_{m2}\right)V_2 + \cdots + \left(\sum_{m=0}^{n} \mathscr{C}_{mn}\right)V_n \\ &+ \left(\sum_{m=0}^{n} \mathscr{C}_{0m} + \sum_{m=0}^{n} \mathscr{C}_{1m} + \cdots + \sum_{m=0}^{n} \mathscr{C}_{nm}\right)\phi_0 \end{aligned} \tag{3.18a}$$

or

$$\phi_0 = -\frac{\displaystyle\sum_{k=1}^{n}\left[\left(\sum_{m=0}^{n} \mathscr{C}_{mk}\right)V_k\right]}{\displaystyle\sum_{l=0}^{n}\left[\sum_{m=0}^{n} \mathscr{C}_{lm}\right]} \tag{3.18b}$$

Substituting (3.18b) into the last n equations in (3.17) yields the entries in the

per-unit-length capacitance matrix, C, given in (3.16) as [C.4]

$$C_{ij} = \mathscr{C}_{ij} - \frac{\left(\sum_{k=0}^{n} \mathscr{C}_{ik}\right)\left(\sum_{m=0}^{n} \mathscr{C}_{mj}\right)}{\left(\sum \mathscr{C}\right)} \tag{3.19}$$

The first summation in the numerator of (3.19) is the *sum of all the elements in the i-th row of* $\mathscr{C}$, whereas the second summation in the numerator of (3.19) is the *sum of all the elements in the j-th column of* $\mathscr{C}$. The denominator summation, $\sum \mathscr{C}$, is the *sum of all the elements in* $\mathscr{C}$.

In the case of two conductors, the result in (3.19) gives the per-unit-length capacitance between the two conductors and reduces to

$$c = \frac{\mathscr{C}_{11}\mathscr{C}_{00} - \mathscr{C}_{01}\mathscr{C}_{10}}{\mathscr{C}_{00} + \mathscr{C}_{01} + \mathscr{C}_{10} + \mathscr{C}_{11}} \tag{3.20}$$

The generalized capacitance matrix, like the transmission-line capacitance, is symmetric so that $\mathscr{C}_{01} = \mathscr{C}_{10}$. Eliminating the potential reference node (or line) and observing that capacitors in series (parallel) combine like resistors in parallel (series) one can directly obtain the result in (3.20) from the equivalent circuit of Fig. 3.7(a).

Therefore we can obtain the per-unit-length *generalized capacitance matrix*, $\mathscr{C}$, choose a reference conductor, and then easily compute C for that choice of reference conductor from $\mathscr{C}$ using the relation in (3.19). If the surrounding medium is inhomogeneous in ε, we similarly compute the generalized capacitance matrix *with the dielectric removed (replaced with free space)*. $\mathscr{C}_o$, and from that compute the per-unit-length capacitance matrix *with the dielectric removed*, $\mathbf{C}_o$, with the above method. Once $\mathbf{C}_o$ is computed in this fashion, we may then compute $\mathbf{L} = \mu\varepsilon_o\mathbf{C}_o^{-1}$.

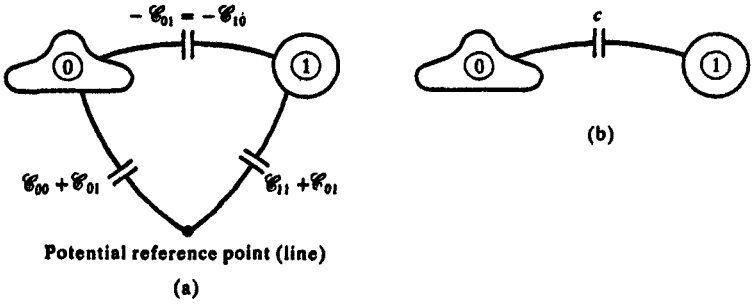

FIGURE 3.7 Illustration of (a) the meaning of the per-unit-length generalized capacitance matrix for a two-conductor line and (b) the elimination of the reference line to yield the capacitance between the conductors.

3.2 MULTICONDUCTOR LINES HAVING CONDUCTORS OF CIRCULAR CYLINDRICAL CROSS SECTION

Conductors having cross sections that are circular cylindrical are referred to as *wires*. These types of conductors are frequently found in cables that interconnect electronic circuitry and form an important class of MTL's [A.3]. These are some of the few conductor types for which simple closed-form equations for the per-unit-length parameters can be obtained.

3.2.1 Fundamental Subproblems for Wires

In order to determine simple relations for the per-unit-length parameters of wires, we need to discuss the following important subproblems [A.3, B.1, 1, 2].

3.2.1.1 Magnetic Flux Due to a Filament of Current Consider a wire carrying a current I that is uniformly distributed over its cross section as shown in Fig. 3.8. The transverse magnetic field intensity, $\vec{\mathscr{H}}_t$, is directed in the circumferential direction by symmetry. Enclosing the wire and current by a cylinder of radius r and applying Ampere's law for the TEM field [A.1]:

$$\oint_c \vec{\mathscr{H}}_t \cdot d\vec{l} = I \tag{3.21}$$

gives

$$\mathscr{H}_t = \frac{I}{2\pi r} \tag{3.22}$$

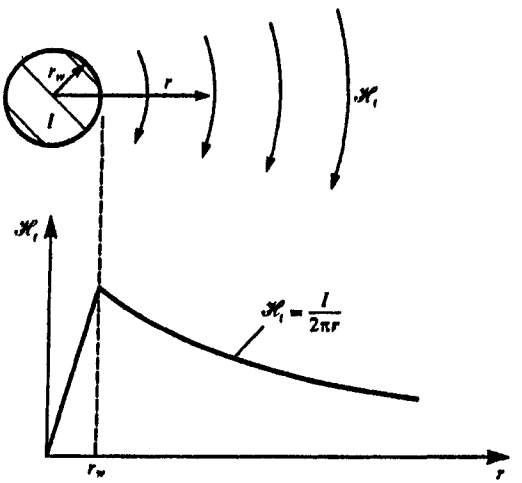

FIGURE 3.8 Magnetic field intensity within and about a current-carrying wire.

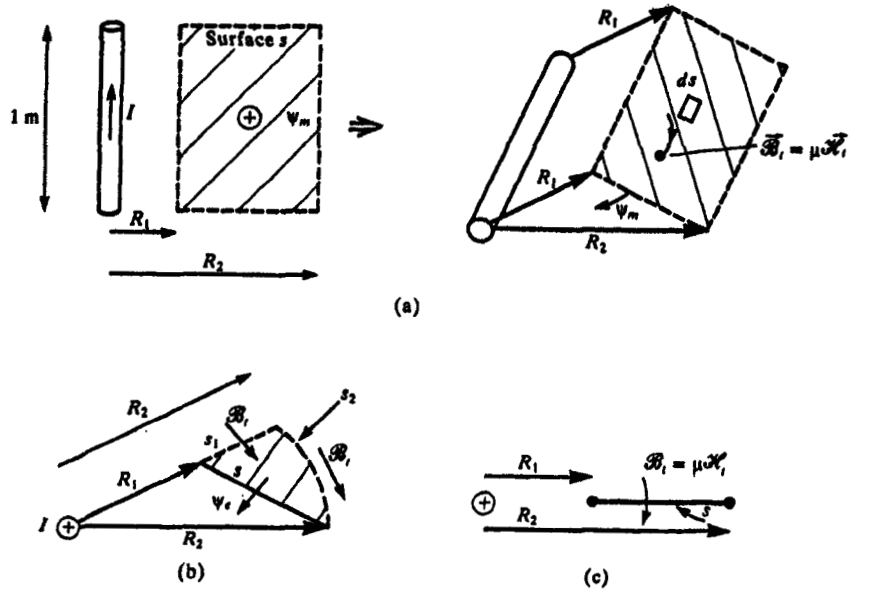

FIGURE 3.9 Illustration of the calculation of magnetic flux through a surface via a simpler problem.

This result is due to the observations that:

1. $\vec{\mathcal{H}}_t$ is tangent to $d\vec{l}$ and therefore the dot product can be removed from (3.21) and the vectors replaced with their magnitudes.
2. $\vec{\mathcal{H}}_t$ is constant around the contour of radius r and so may be removed from the integral.

Now consider determining the magnetic flux from this current that penetrates a surface s that is parallel to the wire and of uniform cross section along the wire length as shown in Fig. 3.9(a). The edges of the surface are at distances R_1 and R_2 from the wire. Next consider this problem in cross section as shown in Fig. 3.9(b). Consider the closed, wedge-shaped surface consisting of the original surface along with surfaces s_1 and s_2. Surface s_1 is the flat surface extending radially along R_1 to a radius of R_2, and surface s_2 is a cylindrical surface of constant radius R_2 that joins surfaces s and s_1. Gauss' law provides that there are no (known) isolated sources of the magnetic field. Thus the total magnetic flux, ψ_m, through a closed surface must be zero [A.1]:

$$\psi_m = \oiint_s \vec{\mathcal{B}} \cdot d\vec{s} = 0 \tag{3.23}$$

where $\vec{\mathscr{B}}$ is the *magnetic flux density vector* and is related for linear, homogeneous, isotropic media to the magnetic field intensity vector, $\vec{\mathscr{H}}$, as $\vec{\mathscr{B}} = \mu\vec{\mathscr{H}}$. From (3.23), the total magnetic flux through the wedge-shaped surface of Fig. 3.9 is the sum of the fluxes through the original surface, s, and surfaces s_1 and s_2 since no flux is directed through the end caps because of the transverse nature of the magnetic field. But the flux through s_2 is also zero because the magnetic field is tangent to it. Thus the total magnetic flux penetrating the original surface s is the same as the flux penetrating surface s_1 as shown in Fig. 3.9(c). But the problem of Fig. 3.9(c) is simpler than the original problem because the magnetic field is orthogonal to the surface. Thus the total magnetic flux through either surface is

$$\begin{aligned}\psi_m &= \oiint_s \vec{\mathscr{B}}_t \cdot d\vec{s} \\ &= \oiint_{s_1} \vec{\mathscr{B}}_t \cdot d\vec{s} \\ &= \Delta z \int_{R_1}^{R_2} \frac{\mu I}{2\pi r}\, dr \\ &= \Delta z \frac{\mu I}{2\pi} \ln\left(\frac{R_2}{R_1}\right)\end{aligned} \tag{3.24}$$

where we have assumed that $R_2 > R_1$ to give the indicated direction of ψ_m. The magnetic flux *per unit of line length* is

$$\frac{\psi_m}{\Delta z} = \frac{\mu I}{2\pi} \ln\left(\frac{R_2}{R_1}\right) \text{ Wb/m} \tag{3.25}$$

We will find the results of this subproblem to be of considerable utility in our future developments.

The above derivation has been made with two important assumptions:

1. The wire is infinitely long.
2. The current is uniformly distributed over the wire cross section or symmetrical about its axis.

The first assumption allows us to assume that the magnetic field is invariant along the direction of the wire axis. The second assumption means that we may replace the wire with a *filamentary current* at its axis on which all the current I is concentrated, and implicitly assumes that there are no closely spaced currents to disturb this symmetry. The effects of this infinitely long filament of current on the flux penetrating the above surface will be unchanged.

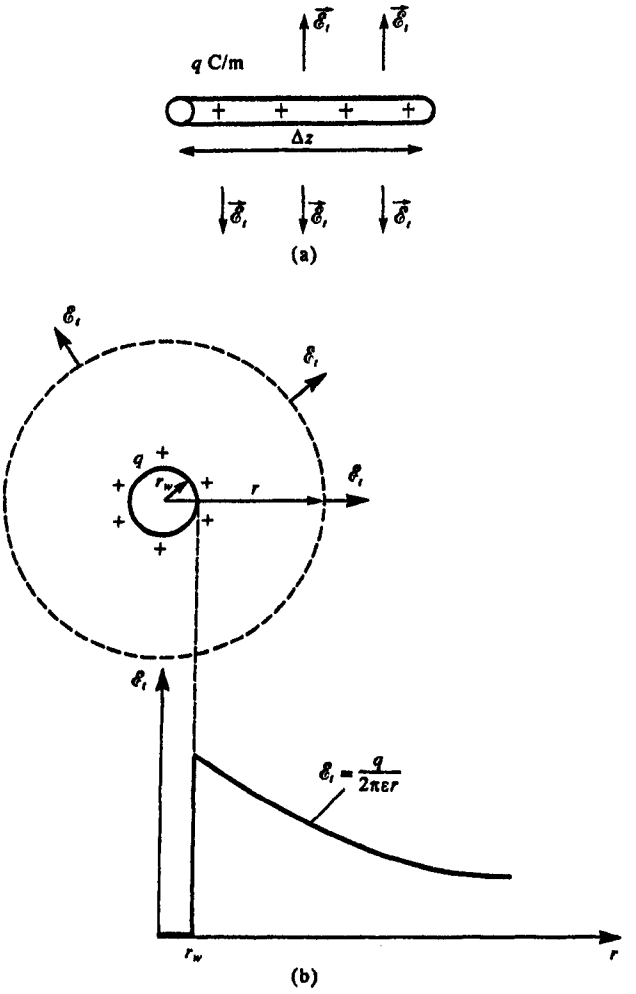

FIGURE 3.10 Illustration of the electric field about a charge-carrying wire.

3.2.1.2 Voltage Due to a Filament of Charge We next consider the dual problem of determining the voltage between two points due to a filament of charge. Consider the very long wire carrying a charge per unit of length q C/m as shown in Fig. 3.10(a). We assume that either the charge is uniformly distributed around the periphery of the wire or concentrated as a filament of charge. In this case, the electric field intensity, $\vec{\mathcal{E}}$, will be radially directed in a direction transverse to the wire. Gauss' law provides that the total electric flux penetrating a closed surface is equal to the net positive charge enclosed by that surface [A.1]:

$$\psi_e = \oiint_s \vec{\mathcal{D}} \cdot d\vec{s} = Q_{\text{enc}} \tag{3.26}$$

where $\vec{\mathscr{D}}$ is the *electric flux density vector.* For linear, homogeneous and isotropic media, this is related to the electric field intensity vector by $\vec{\mathscr{D}} = \varepsilon\vec{\mathscr{E}}$. Consider enclosing the charge-carrying wire with a cylinder of radius r as shown in Fig. 3.10(b). The electric field is obtained by applying (3.26) to that closed surface to yield

$$\varepsilon \oiint_s \vec{\mathscr{E}}_t \cdot d\vec{s} = q\Delta z \tag{3.27}$$

The dot product may be removed and the vectors replaced with their magnitudes since the electric field is orthogonal to the sides of the surface and no electric field is directed through the end caps of the surface. Furthermore, the electric field may be removed from the integral since it is constant in value over the sides of the surface. This gives a simple expression for the electric field away from the filament:

$$\mathscr{E}_r = \frac{q}{2\pi\varepsilon r} \text{ V/m} \tag{3.28}$$

Next consider the problem of determining the voltage between two points away from the filament as shown in Fig. 3.11(a). The points are at radii R_1 and R_2 from the filament. The voltage is defined as (uniquely because of the transverse nature of the electric field)

$$V_{ab} = -\int_c \vec{\mathscr{E}}_t \cdot d\vec{l} \tag{3.29}$$

A simpler problem is illustrated in Fig. 3.11(b). Contour c_1 extends along a radial line from the end of R_1 to a distance R_2, and contour c_2 is of constant radius R_2 and extends from that end to the beginning of the original contour. Thus, since (3.29) is independent of the path taken between the two points, we

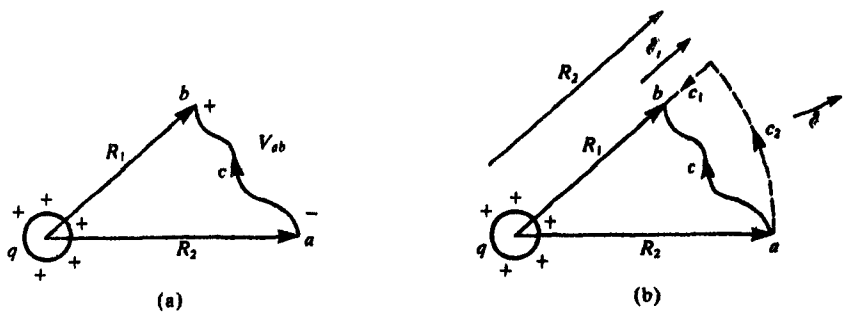

FIGURE 3.11 Illustration of the calculation of voltage of a charge-carrying wire directly and via a simpler problem.

may alternatively compute

$$V_{ab} = -\int_{c_1} \vec{\mathcal{E}}_t \cdot d\vec{l} - \int_{c_2} \vec{\mathcal{E}}_t \cdot d\vec{l} \tag{3.30}$$

$$= -\int_{R_2}^{R_1} \frac{q}{2\pi\varepsilon r}\, dr$$

$$= \frac{q}{2\pi\varepsilon} \ln\left(\frac{R_2}{R_1}\right)$$

This result was made possible by the observation that over c_2 the electric field is orthogonal to the contour so that the second integral is zero, and over c_1 the electric field is tangent to the contour. We will also find this result to be of considerable utility in our future work.

Once again, this simple result implicitly assumes that:

1. The filament is infinitely long.
2. The charge is uniformly distributed around its periphery.

The first assumption ensures that the electric field will not vary along the line length. The second assumption means that we may replace the wire with a filament of charge, and implicitly assumes that there are no closely spaced charge distributions to disturb this symmetry.

3.2.1.3 The Method of Images The last principle that we will employ is the *method of images.* Consider a point charge Q situated a height h above an infinite, perfectly conducting plane as shown in Fig. 3.12(a). We can replace the infinite plane with an equal but negative charge $-Q$ at a distance h below the previous location of the surface of the plane and the resulting fields will be identical in the space above the plane's surface [A.1]. The negative charge is said to be the *image* of the positive charge. We can similarly image currents. Consider a current I parallel to and at a height h above an infinite, perfectly conducting plane shown in Fig. 3.12(b). If the plane is replaced with an equal but oppositely directed current at a distance h below the position of the plane surface, all the fields above the plane's surface will be identical in both problems [A.1]. This can be conveniently remembered using the following mnemonic device. Consider the current I as producing positive charge at one endpoint and negative at the other (denoted by circles with enclosed polarity signs). Imaging these "point charges" in the way described gives the correct image current direction. A vertically directed current is similarly imaged as shown in Fig. 3.12(c). Current directions which are neither vertical nor horizontal can be resolved into their horizontal and vertical components and the above results used to give the correct image current distribution [A.1].

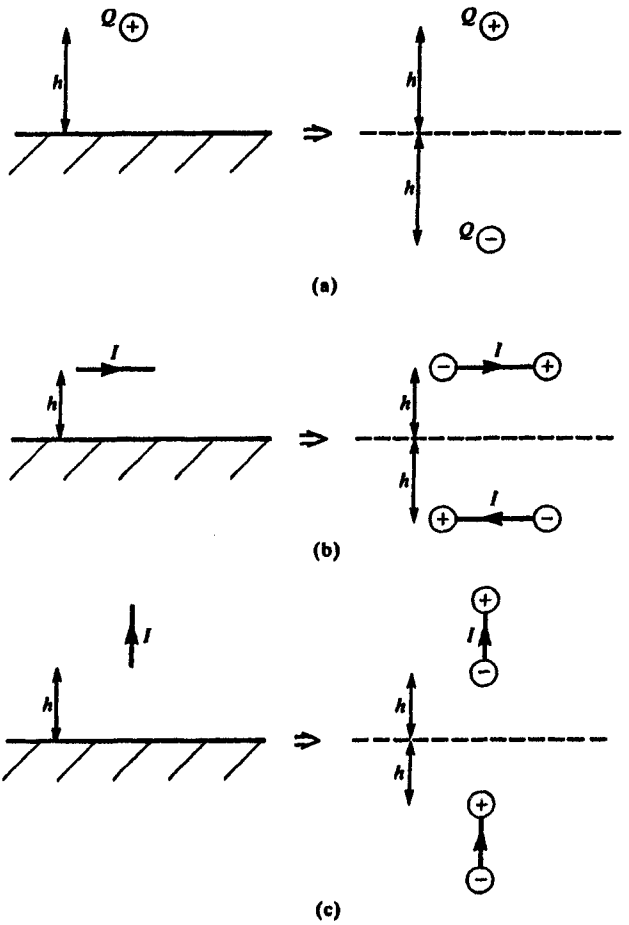

FIGURE 3.12 Illustration of the method of images for (a) a charge above an infinite, perfectly conducting plane, (b) and (c) its extension to current images.

3.2.2 Exact Solutions for Two-Conductor Wire Lines

There exist few transmission-line structures for which the per-unit-length parameters can be determined *exactly*. The class of two-conductor lines of circular cylindrical cross section *in a homogeneous medium* considered in this section represents a significant portion of such lines.

3.2.2.1 Two Wires Consider the case of two wires of radii r_{w1} and r_{w2} as shown in Fig. 3.13(a). Let us assume that the currents are uniformly distributed around the wire peripheries as shown in Fig. 3.13(b). Using the above result for the magnetic flux from a filament of current, we obtain the total flux passing

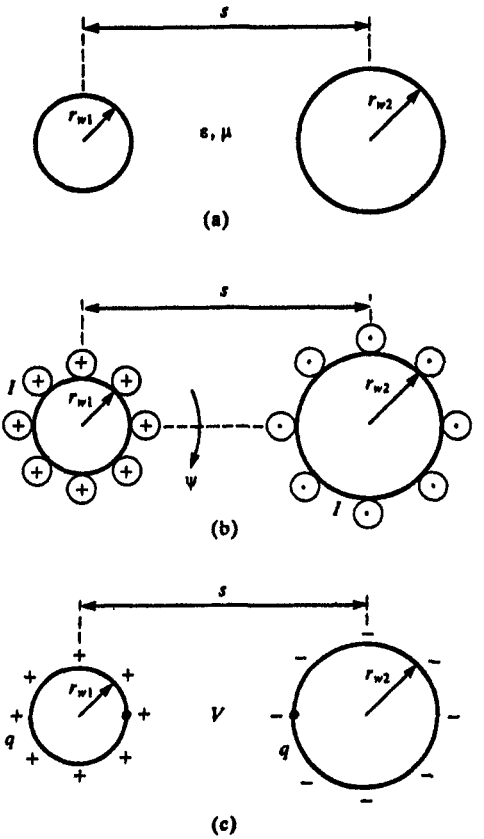

FIGURE 3.13 Illustration of (a) a two-wire line and calculation of (b) the per-unit-length inductance and (c) the per-unit-length capacitance for widely separated wires.

between the two wires as

$$\psi = \frac{\mu I}{2\pi} \ln\left(\frac{s - r_{w2}}{r_{w1}}\right) + \frac{\mu I}{2\pi} \ln\left(\frac{s - r_{w1}}{r_{w2}}\right) \tag{3.31}$$

$$= \frac{\mu I}{2\pi} \ln\left[\frac{(s - r_{w2})(s - r_{w1})}{r_{w1} r_{w2}}\right]$$

This result assumes that the current is uniformly distributed around each wire periphery. This will not be the case if the wires are closely separated since one current will interact and cause a nonuniform distribution of the other current (this is referred to as *proximity effect*). In order to make this result valid, we must require that the wires be *widely separated.* The necessary ratio of separation to wire radius to make this valid will be investigated when we

determine the exact solution. Therefore, because of the necessity to have the wires widely separated, the separation must be much larger than either of the wire radii so that (3.31) simplifies to

$$l = \frac{\psi}{I} \tag{3.32}$$

$$\cong \frac{\mu}{2\pi} \ln\left(\frac{s^2}{r_{w1}r_{w2}}\right) \text{ H/m}$$

In the practical case of the wire radii being equal, $r_{w1} = r_{w2} = r_w$, this reduces to

$$l \cong \frac{\mu}{\pi} \ln\left(\frac{s}{r_w}\right) \text{ H/m} \tag{3.33}$$

The per-unit-length capacitance will be similarly determined in an approximate manner. Consider the two wires carrying charge uniformly distributed around each wire periphery as shown in Fig. 3.13(c). The voltage between the wires can be similarly obtained using (3.30) as

$$V = \frac{q}{2\pi\varepsilon} \ln\left[\frac{(s - r_{w2})(s - r_{w1})}{r_{w1}r_{w2}}\right] \tag{3.34}$$

$$\cong \frac{q}{2\pi\varepsilon} \ln\left(\frac{s^2}{r_{w1}r_{w2}}\right)$$

and we have used the necessary requirement that the wires be widely separated. The per-unit-length capacitance is

$$c = \frac{q}{V} \tag{3.35}$$

$$\cong \frac{2\pi\varepsilon}{\ln\left(\frac{s^2}{r_{w1}r_{w2}}\right)} \text{ F/m}$$

For equal wire radii this simplifies to

$$c \cong \frac{\pi\varepsilon}{\ln\left(\frac{s}{r_w}\right)} \text{ F/m} \tag{3.36}$$

We now turn to an *exact* derivation of these results. The essence of the method is to concentrate the total per-unit-length charge on each wire, q, on

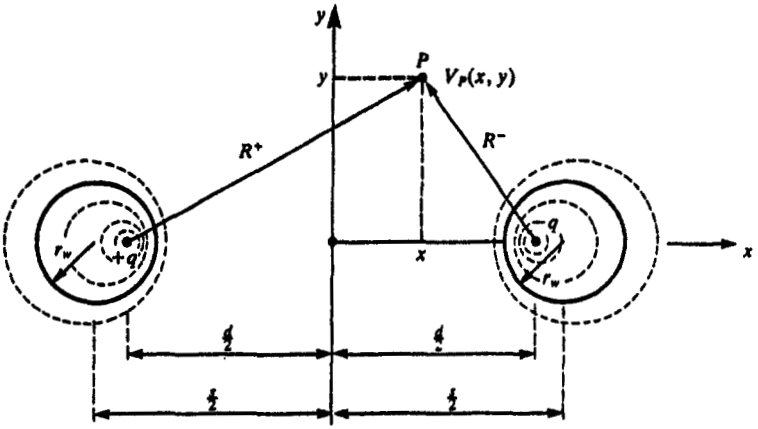

FIGURE 3.14 Illustration of the calculation of the exact per-unit-length capacitance of two wires.

filaments separated a distance d as shown in Fig. 3.14. Then find the *equipotential contours* about these filaments and locate the actual wires on these contours that correspond to the voltages of the wires. This gives the equivalent spacing between the two wires, s, that carry the same charge per unit of line length. The voltage at a point P shown in Fig. 3.14 due to the filaments of charge, one carrying q and the other carrying $-q$, with respect to the origin, $x = 0$ and $y = 0$, can be found using the previous basic subproblem as

$$V_P(x, y) = -\frac{q}{2\pi\varepsilon}\ln\left(\frac{R^+}{d/2}\right) + \frac{q}{2\pi\varepsilon}\ln\left(\frac{R^-}{d/2}\right) \tag{3.37}$$

$$= \frac{q}{2\pi\varepsilon}\ln\left(\frac{R^-}{R^+}\right)$$

Thus points on equipotential contours are such that the ratio

$$\frac{R^-}{R^+} = e^{(2\pi\varepsilon V_P/q)} \tag{3.38}$$

$$= K$$

is constant where K is some constant. Substituting the equations for R^+ and R^-:

$$R^+ = \sqrt{(x + d/2)^2 + y^2} \tag{3.39a}$$

$$R^- = \sqrt{(x - d/2)^2 + y^2} \tag{3.39b}$$

gives

$$\frac{(x - d/2)^2 + y^2}{(x + d/2)^2 + y^2} = K^2 \tag{3.40}$$

Writing (3.40) in the form of the equation for a circle of radius r that is centered at $x = h$, $y = 0$:

$$(x - h)^2 + y^2 = r^2 \tag{3.41a}$$

gives

$$h = \frac{d}{2}\frac{K^2 + 1}{K^2 - 1} \tag{3.41b}$$

$$r = \frac{Kd}{K^2 - 1} \tag{3.41c}$$

The constant K can be eliminated by taking the difference of the squares of (3.41b) and (3.41c) to give

$$\frac{d}{2} = \sqrt{h^2 - r^2} \tag{3.42}$$

The value of potential for each of these equipotential surfaces can be found by solving (3.41) for K to give

$$K = \frac{h}{r} \pm \sqrt{\left(\frac{h}{r}\right)^2 - 1} = \frac{h \pm d}{r} \tag{3.43}$$

Substituting this into (3.38) and solving for the voltage gives

$$V_P = \frac{q}{2\pi\varepsilon} \ln\left[\frac{h}{r} + \sqrt{\left(\frac{h}{r}\right)^2 - 1}\right] \tag{3.44}$$

Recall that this is the voltage of the point *with respect to the origin of the coordinate system* which is located midway between the two wires. Thus the *voltage between the two wires that are separated by distance s is*

$$V = 2V_P = \frac{q}{\pi\varepsilon} \ln\left[\frac{s}{2r_w} + \sqrt{\left(\frac{s}{2r_w}\right)^2 - 1}\right] \tag{3.45}$$

and the per-unit-length capacitance becomes

$$c = \frac{q}{V} \tag{3.46}$$

$$= \frac{\pi\varepsilon}{\ln\left[\frac{s}{2r_w} + \sqrt{\left(\frac{s}{2r_w}\right)^2 - 1}\right]} \text{ F/m}$$

This can be defined in terms of the inverse hyperbolic cosine as

$$\cosh^{-1}(x) = \ln(x + \sqrt{x^2 - 1}) \tag{3.47}$$

to give

$$c = \frac{\pi\varepsilon}{\cosh^{-1}\left(\frac{s}{2r_w}\right)} \text{ F/m} \tag{3.48}$$

If the wire radii are not equal, the corresponding *exact result* for the per-unit-length capacitance is derived in [3] and becomes

$$c = \frac{\pi\varepsilon}{\cosh^{-1}\left(\frac{s^2 - r_{w1}^2 - r_{w2}^2}{2r_{w1}r_{w2}}\right)} \text{ F/m} \tag{3.49}$$

The *exact* result in (3.46) or (3.48) simplifies for widely spaced wires. For example, suppose $s \gg r_w$. The exact result in (3.46) reduces to the approximate result derived earlier and given in (3.36). The error for a ratio $s/r_w = 5$ is only 2.7%. A ratio of separation to wire radius of 4 would mean that another wire of the same radius would just fit between the two original wires. For this very small separation, the error between the approximate expression (3.36) and the exact expression (3.46) is only 5.3%! So the *wide-separation approximation* given in (3.36) is quite adequate for practical wire separations.

The per-unit-length inductance can be obtained from this result, assuming the surrounding medium is *homogeneous* in ε and μ as

$$l = \mu\varepsilon c^{-1} \tag{3.50}$$

$$= \frac{\mu}{\pi}\cosh^{-1}\left(\frac{s}{2r_w}\right) \text{ H/m}$$

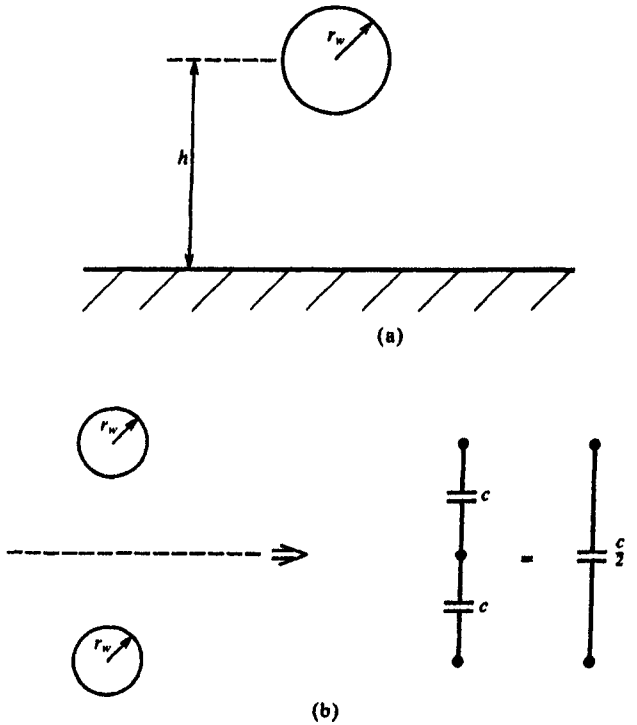

FIGURE 3.15 Determination of the per-unit-length capacitance of one wire above an infinite plane via the method of images.

Similarly, if the medium is lossy and homogeneous in σ we can obtain

$$g = \frac{\sigma}{\varepsilon} c \tag{3.51}$$

$$= \frac{\pi\sigma}{\cosh^{-1}\left(\frac{s}{2r_w}\right)} \text{ S/m}$$

This latter result for the per-unit-length conductance is not particularly realistic since the only reasonably infinite, homogeneous medium that can exist around the two wires is free space which has $\sigma = 0$.

3.2.2.2 One Wire Above an Infinite, Perfectly Conducting Plane Next consider the case of one wire at a height h above and parallel to an infinite, perfectly conducting plane (sometimes referred to as a *ground plane*) as shown in Fig. 3.15(a). By the method of images we may replace the plane with its image located at an equal distance h below the position of the plane as shown in Fig.

3.15(b). The desired capacitance is between each wire and the position of the plane. But, since capacitances in series add like resistors in parallel, we see that this problem can be related to the problem of the previous section as:

$$c_{\text{two wire}} = \frac{c_{\text{one wire above ground}}}{2} \tag{3.52}$$

Therefore the capacitance of one wire above an infinite, perfectly conducting plane becomes, substituting $h = s/2$ in (3.48),

$$c = \frac{2\pi\varepsilon}{\cosh^{-1}\left(\dfrac{h}{r_w}\right)} \text{ F/m} \tag{3.53}$$

or, approximately, for $h \gg r_w$:

$$c \cong \frac{2\pi\varepsilon}{\ln\left(\dfrac{2h}{r_w}\right)} \text{ F/m} \tag{3.54}$$

Similarly, the inductance can be obtained from this result as

$$\begin{aligned} l &= \mu\varepsilon c^{-1} \\ &= \frac{\mu}{2\pi}\cosh^{-1}\left(\frac{h}{r_w}\right) \text{ H/m} \\ &\cong \frac{\mu}{2\pi}\ln\left(\frac{2h}{r_w}\right) \end{aligned} \tag{3.55}$$

3.2.2.3 The Coaxial Cable Consider the *coaxial cable* shown in Fig. 3.16 consisting of a wire of radius r_w within and centered on the axis of a shield of inner radius r_s. The medium between the wire and the shield is assumed to be homogeneous. The case of an inhomogeneous medium can be solved so long as the inhomogeneity exists in annulae symmetric about the shield axis. (See the end-of-chapter Problem 3.1.) If we place a total charge q per unit of line length on the inner conductor, a negative charge of equal magnitude will be induced on the interior of the shield. Observe that *by symmetry, the charge distributions will be uniformly distributed around the conductor peripheries regardless of the conductor separations.* We earlier obtained the result for the electric field due to the charge, q, per unit of line length on the inner wire as

$$\vec{\mathcal{E}}_i = \frac{q}{2\pi\varepsilon r}\,\hat{a}_r \qquad r_w \le r \le r_s \tag{3.56}$$

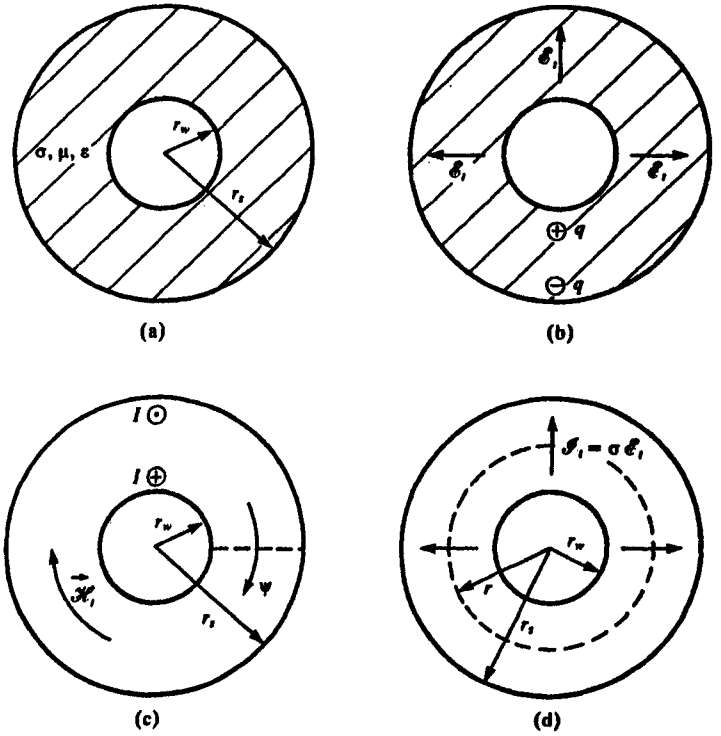

FIGURE 3.16 Calculation of the per-unit-length parameters for a coaxial cable: (a) the general structure, (b) capacitance, (c) inductance, and (d) conductance.

Observe that the field will be directed in the radial (transverse) direction. The voltage between the two conductors can be obtained as

$$V = -\int_{r_s}^{r_w} \frac{q}{2\pi\varepsilon r}\, dr \tag{3.57}$$

$$= \frac{q}{2\pi\varepsilon} \ln\left(\frac{r_s}{r_w}\right)$$

The capacitance per unit of line length is therefore

$$c = \frac{q}{V} \tag{3.58}$$

$$= \frac{2\pi\varepsilon}{\ln\left(\dfrac{r_s}{r_w}\right)} \text{ F/m}$$

Observe that, because of symmetry, the charge distributions will be uniform around the conductor peripheries regardless of conductor separation so that this result is *exact*. The per-unit-length inductance can be derived directly or by using

$$l = \mu\varepsilon c^{-1} \tag{3.59}$$

$$= \frac{\mu}{2\pi} \ln\left(\frac{r_s}{r_w}\right) \text{ H/m}$$

Similarly, the per-unit-length conductance is

$$g = \frac{\sigma}{\varepsilon} c \tag{3.60}$$

$$= \frac{2\pi\sigma}{\ln\left(\frac{r_s}{r_w}\right)} \text{ S/m}$$

The per-unit-length inductance can be derived directly. Consider placing a flat surface of length Δz between the inner and outer conductors as shown in Fig. 3.16(c). The desired magnetic flux passes through this surface. Clearly the flux will be in the circumferential direction since, due to symmetry, the current will be uniformly distributed around the periphery of the inner wire and the inside of the shield. Thus we may use the fundamental result derived earlier to give

$$l = \frac{\psi}{I} \tag{3.61}$$

$$= \frac{\mu}{2\pi} \ln\left(\frac{r_s}{r_w}\right)$$

The per-unit-length conductance given in (3.60) can similarly be obtained directly from Fig. 3.16(d) by finding the ratio of the transverse current to the voltage:

$$g = \frac{\int_{\phi=0}^{2\pi} \sigma \mathscr{E}_t r \, d\phi}{V} \tag{3.62}$$

$$= \frac{2\pi\sigma}{\ln\left(\frac{r_s}{r_w}\right)}$$

3.2.3 Wide-Separation Approximations for Wires in Homogeneous Media

The above results for two-conductor lines in a homogeneous medium are exact. For similar lines consisting of more than two conductors, exact closed-form

solutions cannot be obtained, in general. However, if the wires are relatively widely spaced, we can obtain some simple but approximate closed-form solutions using the fundamental subproblems derived in Section 3.2.1 [B.1]. These results assume that the currents and charges are uniformly distributed around the wire peripheries which implicitly assumes that the wires are widely spaced. As we saw in the case of two-wire lines, the requirement of *widely spaced wires* is not overly restrictive. The following wide-separation approximations for wires are implemented in the FORTRAN program **WIDESEP.FOR** described in Appendix A.

3.2.3.1 (n + 1) Wires Consider the case of $(n + 1)$ wires in a homogeneous medium as shown in Fig. 3.17(a). The entries in the per-unit-length inductance are defined in (3.2). If the wires are widely separated, we can use the fundamental subproblems derived in Section 3.2.1 to give these entries. The self-inductance is obtained from Fig. 3.17(b) as

$$l_{ii} = \left.\frac{\psi_i}{I_i}\right|_{I_1=\cdots=I_{i-1}=I_{i+1}=\cdots=I_n=0} \tag{3.63a}$$

$$= \frac{\mu}{2\pi}\ln\left(\frac{d_{i0}}{r_{w0}}\right) + \frac{\mu}{2\pi}\ln\left(\frac{d_{i0}}{r_{wi}}\right)$$

$$= \frac{\mu}{2\pi}\ln\left(\frac{d_{i0}^2}{r_{w0}r_{wi}}\right)$$

$$l_{ij} = \left.\frac{\psi_i}{I_j}\right|_{I_1=\cdots=I_{j-1}=I_{j+1}=\cdots=I_n=0} \tag{3.63b}$$

$$= \frac{\mu}{2\pi}\ln\left(\frac{d_{j0}}{d_{ij}}\right) + \frac{\mu}{2\pi}\ln\left(\frac{d_{i0}}{r_{w0}}\right)$$

$$= \frac{\mu}{2\pi}\ln\left(\frac{d_{i0}d_{j0}}{d_{ij}r_{w0}}\right)$$

The entries in the per-unit-length capacitance and conductance matrices can be obtained from this result as

$$\mathbf{C} = \mu\varepsilon\mathbf{L}^{-1} \tag{3.64}$$

$$\mathbf{G} = \frac{\sigma}{\varepsilon}\mathbf{C} \tag{3.65}$$

$$= \sigma\mu\mathbf{L}^{-1}$$

3.2.3.2 n Wires Above an Infinite, Perfectly Conducting Plane Consider the case of n wires above and parallel to an infinite, perfectly conducting plane shown

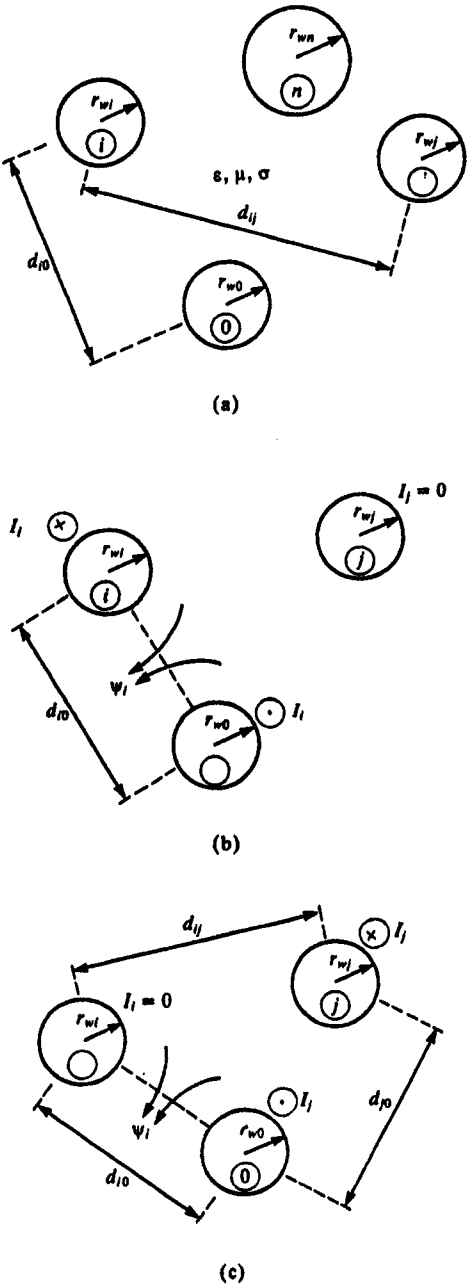

FIGURE 3.17 Illustration of the calculation of per-unit-length inductances using the wide-separation approximations for $(n + 1)$ wires: (a) the cross-sectional structure, (b) self-inductance, and (c) mutual inductance.

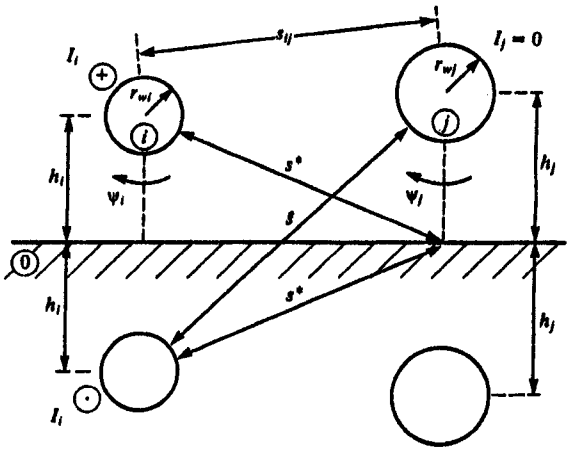

FIGURE 3.18 Illustration of the calculation of per-unit-length inductances using the wide-separation approximations for n wires above a ground plane.

in Fig. 3.18. Replacing the plane with the image currents and using the fundamental result derived in Section 3.2.1 yields

$$l_{ii} = \left.\frac{\psi_i}{I_i}\right|_{I_1=\cdots=I_{i-1}=I_{i+1}=\cdots=I_n=0} \tag{3.66a}$$

$$= \frac{\mu}{2\pi}\ln\left(\frac{h_i}{r_{wi}}\right) + \frac{\mu}{2\pi}\ln\left(\frac{2h_i}{h_i}\right)$$

$$= \frac{\mu}{2\pi}\ln\left(\frac{2h_i}{r_{wi}}\right)$$

$$l_{ij} = l_{ji} = \left.\frac{\psi_j}{I_i}\right|_{I_1=\cdots=I_{i-1}=I_{i+1}=\cdots=I_n=0} \tag{3.66b}$$

$$= \frac{\mu}{2\pi}\ln\left(\frac{s^*}{s_{ij}}\right) + \frac{\mu}{2\pi}\ln\left(\frac{s}{s^*}\right)$$

$$= \frac{\mu}{2\pi}\ln\left(\frac{\sqrt{s_{ij}^2 + 4h_ih_j}}{s_{ij}}\right)$$

$$= \frac{\mu}{4\pi}\ln\left(1 + \frac{4h_ih_j}{s_{ij}^2}\right)$$

The entries in the per-unit-length capacitance and conductance matrices can then be found from these results using (3.64) and (3.65).

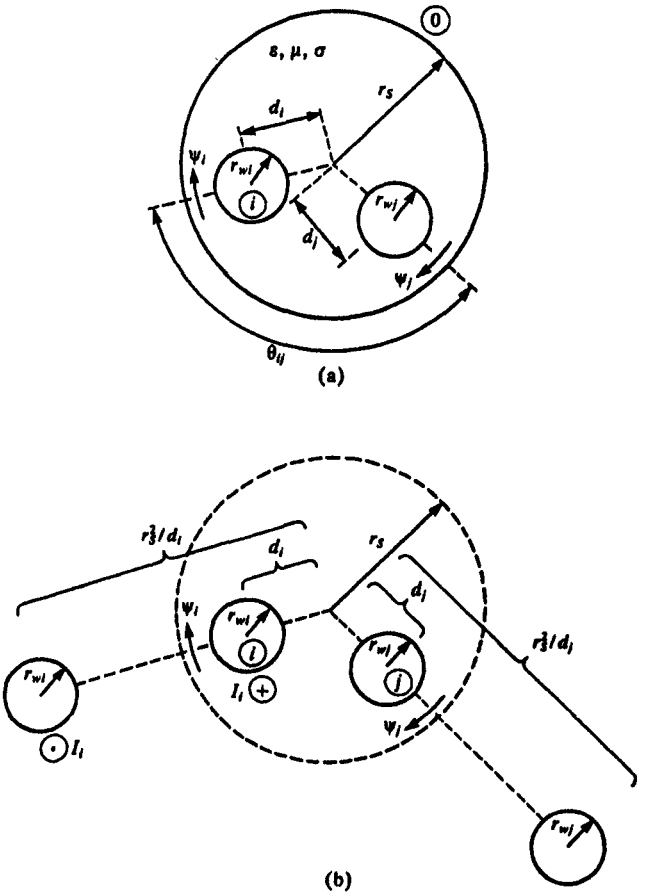

FIGURE 3.19 Illustration of the calculation of per-unit-length inductances using the wide-separation approximations for n wires within a cylindrical shield: (a) the cross-sectional structure, (b) replacement with images.

3.2.3.3 n Wires Within a Perfectly Conducting Shield Consider n wires of radii r_{wi} within a perfectly conducting, circular cylindrical shield shown in Fig. 3.19(a). The interior radius of the shield is denoted by r_S and the distances of the wires from the shield axis are denoted by d_i while the angular separations are denoted by θ_{ij}. The perfectly conducting shield may be replaced by image currents located at radial distances from the shield center of r_S^2/d_i as shown in Fig. 3.19(b) [2, 3]. The directions of the desired magnetic fluxes are as shown. Assuming the wires are widely separated from each other and the shield, we may assume that the currents are uniformly distributed around the wire and shield peripheries. Thus we may use the basic results of Section 3.2.1 to

give

$$l_{ii} = \left.\frac{\psi_i}{I_i}\right|_{I_1=\cdots=I_{i-1}=I_{i+1}=\cdots=I_n=0} \tag{3.67a}$$

$$= \frac{\mu}{2\pi}\ln\left(\frac{r_S - d_i}{r_{wi}}\right) + \frac{\mu}{2\pi}\ln\left(\frac{r_S^2/d_i - d_i}{r_S^2/d_i - r_S}\right)$$

$$= \frac{\mu}{2\pi}\ln\left(\frac{r_S^2 - d_i^2}{r_S r_{wi}}\right)$$

$$l_{ij} = l_{ji} = \left.\frac{\psi_j}{I_i}\right|_{I_1=\cdots=I_{i-1}=I_{i+1}=\cdots=I_n=0} \tag{3.67b}$$

$$= \frac{\mu}{2\pi}\ln\left[\frac{d_j}{r_S}\sqrt{\frac{(d_i d_j)^2 + r_S^4 - 2d_i d_j r_S^2\cos\theta_{ij}}{(d_i d_j)^2 + d_j^4 - 2d_i d_j^3\cos\theta_{ij}}}\right]$$

The entries in the per-unit-length capacitance and conductance matrices can then be found from these results using (3.64) and (3.65).

3.2.4 Numerical Methods for the General Case

The above results assumed that the medium surrounding the wires is homogeneous. For two wires or one wire above a ground plane, closed-form results have not been obtained for an inhomogeneous surrounding medium. For the coaxial cable, exact results can be obtained for an inhomogeneous medium so long as it is symmetric with respect to the shield axis. (See Problem 3.1 at the end of the chapter.) In the case of wire lines consisting of more than two conductors, exact results cannot be obtained even for a homogeneous surrounding medium, and wide-separation approximations must be used. There are some special cases for infinite structures of wires for which exact solutions can be obtained but these are not realistic for MTL applications [2, 3]. In this section we will discuss a numerical approximation technique which can be used to obtain accurate results for multiwire lines for an inhomogeneous surrounding medium as well as closely spaced conductors. The importance of considering wires that are immersed in inhomogeneous media stems from the practical requirement that circular cylindrical dielectric insulations must surround wire conductors to prevent shorting of the conductors. Closely spaced wires occur in many practical applications. An example is the use of ribbon cables wherein a group of dielectric-insulated wires are maintained in close proximity in a plane. The following method for dealing with these types of problems is described in [C.1–C.7].

Consider an $(n + 1)$-wire line in a homogeneous medium. If the wires are closely spaced, proximity effect will cause the charge and current distributions around the wire peripheries to be nonuniform. With the exception of the

two-wire line, this variation was ignored and assumed to be uniform around the wire peripheries. In the case of two wires that are closely spaced, the charge and current distributions will tend to concentrate on the adjacent surfaces (proximity effect). To model this effect, we could assume a *form* of the charge/current distribution around the i-th wire periphery in the form of a Fourier series in the peripheral angle, θ_i, such as

$$\rho_i = \sum_{k=0}^{N_i} \alpha_{ik} f_{ik}(\theta_i) \tag{3.68a}$$

$$= \alpha_{i0} + \sum_{k=1}^{N_i} \alpha_{ik} f_{ik}(\theta_i) \text{ C/m}^2$$

where

$$f_{i0} = 1 \tag{3.68b}$$

$$f_{ik}(\theta_i) = \cos(k\theta_i), \sin(k\theta_i) \; k = 1, \ldots, N_i \tag{3.68c}$$

and the $(N_i + 1)$ *expansion coefficients*, α_{ik}, are determined to satisfy the boundary condition that the potential at points on each conductor *due to all charge distributions* equals the potential of that conductor. The charge distribution in (3.68a) has dimensions of C/m^2 since it gives the distribution around the wire periphery per unit of line length. The total charge on the i-th conductor per unit of line length is obtained by integrating (3.68a) around the wire periphery to yield

$$q_i = \int_{\theta_i=0}^{2\pi} \rho_i r_{wi} \, d\theta_i \tag{3.69}$$

$$= 2\pi r_{wi} \alpha_{i0}$$

This simple result is due to the fact that $\int_{\theta_i=0}^{2\pi} \cos(k\theta_i) \, d\theta_i = \int_{\theta_i=0}^{2\pi} \sin(k\theta_1) \, d\theta_i = 0$.

We now determine the potential at an arbitrary point in the transverse plane at a position r, θ from each of these charge distributions, i.e., $\phi_i(r_p, \theta_p)$, as illustrated in Fig. 3.20(a). This can best be obtained by assuming the charge distribution around the periphery of the conductor is composed of filaments of charge, q, each of whose amplitudes are weighted by the particular distribution, i.e., 1, $\cos(k\theta_i)$, $\sin(k\theta_i)$. Then we use the previous result given in equation (3.30) for the voltage between two points. With reference to Fig. 3.20(b) we obtain

$$\phi_i(r_p, \theta_p) - \phi_0(r_0, \theta_0) = -\frac{q}{2\pi\varepsilon} \ln\left(\frac{s_p}{s_0}\right) \tag{3.70}$$

It was shown in [C.5] that the *potential* of the reference point, $\phi_0(r_0, \theta_0)$, may be omitted *if the system of conductors is electrically neutral, i.e., the net charge per unit of line length is zero.* Since this is satisfied for our MTL systems, we will henceforth omit the reference potential term. Thus the differential

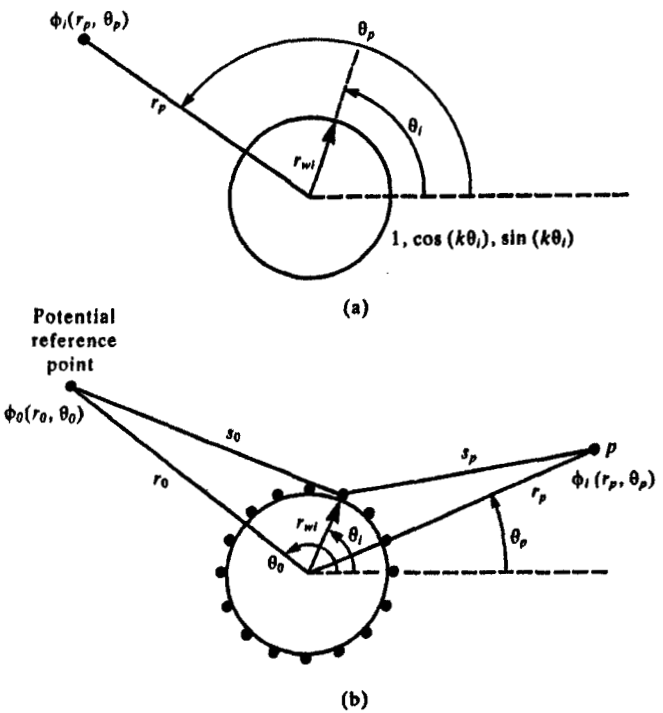

FIGURE 3.20 Determination of the potential of a charge-carrying wire having various circumferential distributions: (a) definition of the problem and (b) replacement of the charge with weighted filaments of charge.

contribution to the potential due to a filamentary component of the charge distribution is

$$d\phi_i(r_p, \theta_p) = -\frac{q}{2\pi\varepsilon} \ln(s_p) \tag{3.71}$$

where the weighted charge distributions are given by

$$q = \rho_i r_{wi}\, d\theta_i \tag{3.72}$$

and the assumed charge distributions are

$$\rho_i = \alpha_{i0} + \sum_{k=1}^{A_i} a_{ik} \cos(k\theta_i) + \sum_{k=1}^{B_i} b_{ik} \sin(k\theta_i) \tag{3.73}$$

with $N_i + 1 = 1 + A_i + B_i$. The distance from the filament to the point is

(according to the law of cosines) given by

$$s_p = \sqrt{r_p^2 + r_{wi}^2 - 2r_p r_{wi}\cos(\theta_i - \theta_p)} \tag{3.74}$$

Substituting these into (3.71) and integrating around the conductor periphery gives the total contribution to the potential due to the charge distributions:

$$\phi_i(r_p, \theta_p) = \alpha_{i0}\int_{\theta_i=0}^{2\pi} I(\theta_i)\,d\theta_i + \sum_{k=1}^{A_i} a_{ik}\int_{\theta_i=0}^{2\pi} I(\theta_i)\cos(\theta_i)\,d\theta_i \tag{3.75a}$$
$$+ \sum_{k=1}^{B_i} b_{ik}\int_{\theta_i=0}^{2\pi} I(\theta_i)\sin(\theta_i)\,d\theta_i$$

where

$$I(\theta_i) = -\frac{1}{2\pi\varepsilon}\ln[\sqrt{r_p^2 + r_{wi}^2 - 2r_p r_{wi}\cos(\theta_i - \theta_p)}] \tag{3.75b}$$
$$= -\frac{1}{4\pi\varepsilon}\ln[r_p^2 + r_{wi}^2 - 2r_p r_{wi}\cos(\theta_i - \theta_p)]$$

Each of the integrals in (3.75a) can be evaluated in closed form giving [B.1]

$$\phi_i(r_p, \theta_p) = \alpha_{i0}\left[-\frac{r_{wi}\ln(r_p)}{\varepsilon}\right] + \sum_{k=1}^{A_i} a_{ik}\left[\frac{r_{wi}^{k+1}\cos(k\theta_p)}{2k\varepsilon r_p^k}\right] \tag{3.76}$$
$$+ \sum_{k=1}^{B_i} b_{ik}\left[\frac{r_{wi}^{k+1}\sin(k\theta_p)}{2k\varepsilon r_p^k}\right]$$

Therefore, the contributions to the potential from each of these charge distributions are given in Table 3.1.

TABLE 3.1 Potential Due to Sinusoidal Charge Expansions

Charge distribution	Contribution to the potential $\phi(r_p, \theta_p)$
1	$-\dfrac{r_w\ln(r_p)}{\varepsilon}$
$\cos(m\theta)$	$\dfrac{r_w^{m+1}\cos(m\theta_p)}{2\varepsilon m r_p^m}$
$\sin(m\theta)$	$\dfrac{r_w^{m+1}\sin(m\theta_p)}{2\varepsilon m r_p^m}$

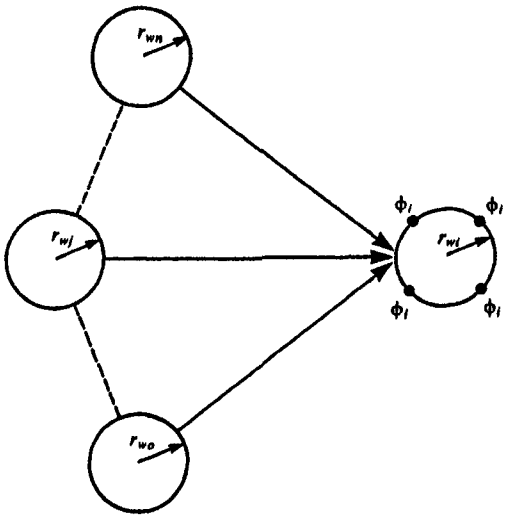

FIGURE 3.21 Determination of the total potential at a point due to all charge distributions.

Satisfaction of the boundary conditions is obtained if we choose a total of

$$N = \sum_{k=0}^{n} (N_k + 1) \tag{3.77}$$

$$= (n + 1) + \sum_{k=0}^{n} A_k + \sum_{k=0}^{n} B_k$$

points on the wires at which we enforce the potential of the wire due to *all the charge distributions on this conductor and all of the other conductors* as illustrated in Fig. 3.21. This leads to a set of N simultaneous equations which must be solved for the expansion coefficients as

$$\mathbf{\Phi} = \mathbf{DA} \tag{3.78a}$$

or, in expanded form,

$$\begin{bmatrix} \Phi_0 \\ \vdots \\ \Phi_i \\ \vdots \\ \Phi_n \end{bmatrix} = \begin{bmatrix} D_{00} & \cdots & D_{0j} & \cdots & D_{0n} \\ \vdots & \vdots & \vdots & \vdots & \vdots \\ D_{i0} & \cdots & D_{ij} & \cdots & D_{in} \\ \vdots & \vdots & \vdots & \vdots & \vdots \\ D_{n0} & \cdots & D_{nj} & \cdots & D_{nn} \end{bmatrix} \begin{bmatrix} A_0 \\ \vdots \\ A_j \\ \vdots \\ A_n \end{bmatrix} \tag{3.78b}$$

The vector of potentials at the matchpoints on the i-th conductor is denoted as

$$\mathbf{\Phi}_i = \begin{bmatrix} \phi_1 \\ \vdots \\ \phi_i \\ \vdots \\ \phi_{i_{N_i}} \end{bmatrix} \tag{3.78c}$$

and the vector of expansion coefficients of the charge distribution on the i-th conductor is denoted as

$$\mathbf{A}_i = \begin{bmatrix} \alpha_{i0} \\ \vdots \\ \alpha_{ik} \\ \vdots \\ \alpha_{iN_i} \end{bmatrix} \tag{3.78d}$$

Inverting (3.78b) gives

$$\mathbf{A} = \mathbf{D}^{-1}\mathbf{\Phi} \tag{3.79a}$$

or, in expanded form,

$$\begin{bmatrix} \mathbf{A}_0 \\ \vdots \\ \mathbf{A}_i \\ \vdots \\ \mathbf{A}_n \end{bmatrix} = \begin{bmatrix} \mathbf{B}_{00} & \cdots & \mathbf{B}_{0j} & \cdots & \mathbf{B}_{0n} \\ \vdots & \vdots & \vdots & \vdots & \vdots \\ \mathbf{B}_{i0} & \cdots & \mathbf{B}_{ij} & \cdots & \mathbf{B}_{in} \\ \vdots & \vdots & \vdots & \vdots & \vdots \\ \mathbf{B}_{n0} & \cdots & \mathbf{B}_{nj} & \cdots & \mathbf{B}_{nn} \end{bmatrix} \begin{bmatrix} \mathbf{\Phi}_0 \\ \vdots \\ \mathbf{\Phi}_j \\ \vdots \\ \mathbf{\Phi}_n \end{bmatrix} \tag{3.79b}$$

The *generalized capacitance matrix*, $\mathscr{C}$, described in Section 3.1.4 can be obtained from (3.79), using (3.69), as [C.1–C.7]

$$\mathscr{C}_{ij} = 2\pi r_{wi} \sum_{\substack{\text{first} \\ \text{row}}} \mathbf{B}_{ij} \tag{3.80}$$

This simple result is due to the fact that, according to (3.69) we only need to

determine α_{i0}, and from (3.79),

$$\begin{bmatrix} \alpha_{i0} \\ \vdots \\ \alpha_{ik} \\ \vdots \\ \alpha_{iN_i} \end{bmatrix} = [\mathbf{B}_{ij}] \begin{bmatrix} \phi_j \\ \vdots \\ \phi_j \\ \vdots \\ \phi_j \end{bmatrix} \tag{3.81}$$

or, in expanded form,

$$\begin{aligned} \alpha_{i0} &= [\mathbf{B}_{ij}]_{11}\phi_j + \cdots + [\mathbf{B}_{ij}]_{1k}\phi_j + \cdots + [\mathbf{B}_{ij}]_{1(N_i+1)}\phi_j \\ &= \{[\mathbf{B}_{ij}]_{11} + \cdots + [B_{ij}]_{1k} + \cdots + [B_{ij}]_{1(N_i+1)}\}\phi_j \end{aligned} \tag{3.82}$$

where $[\mathbf{B}_{ij}]_{mn}$ denotes the entry in row m and column n of $\mathbf{B}_{ij}$.

3.2.4.1 Applications to Inhomogeneous Dielectric Media This method can be extended to handle inhomogeneous media such as circular cylindrical dielectric insulations around the wires by imposing the additional boundary condition that the normal components of the electric flux density vector, $\vec{\mathscr{D}}$, be continuous across the free-space–dielectric and dielectric–conductor interfaces [C.1–C.7]. To illustrate that application, we need to discuss the concepts of *free charge* and *bound charge.*

Dielectric media consist of microscopic dipoles of *bound charge.* In *polar dielectrics,* such as water, the centers of positive and negative electric charge are separated slightly to give microscopic dipoles as illustrated in Fig. 3.22(a). However, any microscopic volume is electrically neutral. In *nonpolar dielectrics,* application of an external electric field causes the charges to separate to give these infinitesimal dipoles. In either case, application of an external electric field causes these microscopic dipoles of *bound charge* to align with the field as illustrated in Fig. 3.22(b). If a slab of dielectric is immersed in an electric field,

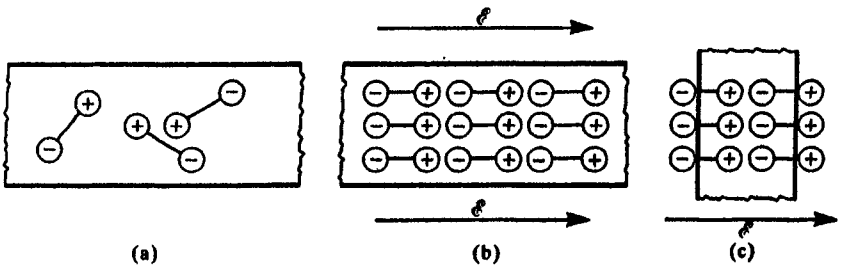

FIGURE 3.22 Illustration of the effects of bound (polarization) charge: (a) microscopic dipoles, no external field (b) alignment of the dipoles with an applied electric field, and (c) creation of a bound surface charge.

a bound charge density will appear on the surfaces of the dielectric as illustrated in Fig. 3.22(c).

For high-frequency variation of the electric field, the charge dipoles cannot align instantaneously with the changes in direction of the electric field but lag behind it. This gives rise to a *polarization loss* which gives the same result as *conduction loss* due to a nonzero conductivity of the dielectric (usually small) [A.1]. To account for both of these losses it is usually the practice to define an *effective conductivity* of the dielectric that includes both these losses in the following manner [A.1]. The sum of conductive and displacement currents in Ampere's law for sinusoidal variation of the electric field is $(\sigma + j\omega\varepsilon)\vec{\mathscr{E}}$. To account for polarization loss, the permittivity is written as the sum of a real and an imaginary part as $\varepsilon = \varepsilon' - j\varepsilon''$. Substituting gives $\sigma + j\omega\varepsilon = (\sigma + \omega\varepsilon'') + j\omega\varepsilon'$ so that the *effective conductivity* is $\sigma_{\text{eff}} = (\sigma + \omega\varepsilon'')$. Thus in any of our uses of σ we intend that to mean the effective conductivity which includes both conductive and polarization losses.

Charge consists of two types: *free charge* is that which is free to move and *bound charge* is the charge appearing on the surfaces of dielectrics in response to an applied electric field as shown in Fig. 3.22(c) which is not free to move. The lines of electric field intensity, $\vec{\mathscr{E}}$, begin and end on both *free charge* and *bound charge*, whereas the lines of electric flux density, $\vec{\mathscr{D}}$, begin and end only on free charge [A.1]. At the interface between two dielectric surfaces the boundary condition is that *the normal components of the electric flux density vector, $\vec{\mathscr{D}}$, must be continuous, i.e.,* $\mathscr{D}_{1n} = \varepsilon_1\mathscr{E}_{1n} = \varepsilon_2\mathscr{E}_{2n} = \mathscr{D}_{2n}$. A simple way of handling inhomogeneous dielectric media is to replace the dielectrics with free space having bound charge at the interface [C.1–C.7]. At places where the dielectric is adjacent to a perfect conductor, we have *both free charge and bound charge* and the free charge density on the surface of the conductor is equal to the component of the electric flux density vector that is normal to the conductor surface, $\sigma = \mathscr{D}_n$ C/m^2, [A.1]. Of course, the component of the electric field intensity vector that is tangent to a boundary is continuous across the boundary for an interface between two dielectrics, $\mathscr{E}_{t1} = \mathscr{E}_{t2}$, and is zero at the surface of a perfect conductor.

In order to adapt the above numerical method to wires that have circular, cylindrical dielectric insulations, we describe the charge (bound plus free) around the wire periphery as a Fourier series in the peripheral angle, θ, as in (3.68):

$$\begin{aligned}\rho_{lf} - \rho_{lb} &= \sum_{k=0}^{N_l} \alpha_{lk} f_{lk}(\theta_l) \qquad (3.83)\\ &= \alpha_{l0} + \sum_{k=1}^{N_l} \alpha_{lk} f_{lk}(\theta_l)\\ &= \alpha_{l0} + \sum_{k=1}^{A_l} a_{lk}\cos(\theta_l) + \sum_{k=1}^{B_l} b_{lk}\sin(\theta_l)\ \text{C/m}^2\end{aligned}$$

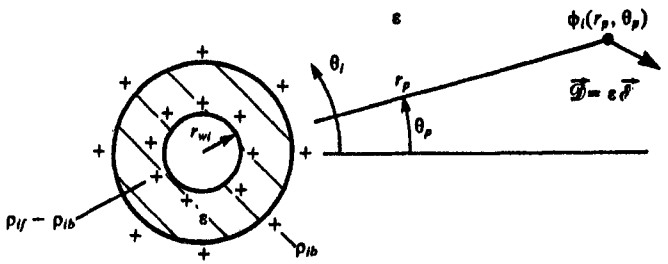

FIGURE 3.23 The general problem of the determination of the potential of a dielectric-insulated wire due to free and bound charge distributions at the two interfaces.

where the expansion or basis functions are again

$$f_{ik}(\theta_i) = 1, \cos(k\theta_i), \sin(k\theta_i) \tag{3.84}$$

In (3.83), ρ_{if} denotes the *free charge distribution* on the i-th conductor periphery and ρ_{ib} denotes the *bound charge distribution* on the dielectric periphery facing the conductor as shown in Fig. 3.23. At the dielectric periphery facing the free-space region, there is only bound charge, which we similarly expand in a Fourier series in peripheral angle as

$$\begin{aligned}\rho_{ib} &= \sum_{k=0}^{\hat{N}_i} \hat{\alpha}_{ik} f_{ik}(\theta_i) \\ &= \hat{\alpha}_{i0} + \sum_{k=1}^{\hat{N}_i} \hat{\alpha}_{ik} f_{ik}(\theta_i) \\ &= \hat{\alpha}_{i0} + \sum_{k=1}^{\hat{A}_i} \hat{a}_{ik} \cos(\theta_i) + \sum_{k=1}^{\hat{B}_i} \hat{b}_{ik} \sin(\theta_i) \text{ C/m}^2\end{aligned} \tag{3.85}$$

In (3.83) we have anticipated that the bound charge distribution around the conductor periphery will be opposite in sign to the bound charge distribution around the dielectric–free-space boundary. For each dielectric-insulated wire, there are a total of $(N_i + 1)$ unknown expansion coefficients, α_{ik}, for the free plus bound charge on the conductor peripheries and a total of $(\hat{N}_i + 1)$ unknown expansion coefficients, $\hat{\alpha}_{ik}$, for the bound charge on the outer dielectric periphery. For a total of $(n + 1)$ wires, this gives a total number of unknowns of $N + \hat{N}$ where

$$\begin{aligned}N &= \sum_{k=0}^{n} (N_k + 1) \\ &= (n + 1) + \sum_{k=0}^{n} A_k + \sum_{k=0}^{n} B_k\end{aligned} \tag{3.86a}$$

$$\hat{N} = \sum_{k=0}^{n} (\hat{N}_k + 1) \tag{3.86b}$$

$$= (n+1) + \sum_{k=0}^{n} \hat{A}_k + \sum_{k=0}^{n} \hat{B}_k$$

unknowns.

In order to enforce the boundary conditions we choose points on each conductor periphery at which to enforce the conductor potential, ϕ_l, and points on each dielectric–free-space periphery at which to enforce the continuity of the normal components of the electric flux density vector due to all these charge distributions. This gives a set of $N + \hat{N}$ simultaneous equations of a form similar to (3.78):

$$\begin{bmatrix} \Phi \\ 0 \end{bmatrix} = \begin{bmatrix} \mathbf{D}_{11} & \mathbf{D}_{12} \\ \mathbf{D}_{21} & \mathbf{D}_{22} \end{bmatrix} \begin{bmatrix} \mathbf{A} \\ \hat{\mathbf{A}} \end{bmatrix} \tag{3.87}$$

The first $N = \sum_{k=0}^{n} (N_k + 1)$ rows enforce the conductor potentials and the second $\hat{N} = \sum_{k=0}^{n} (\hat{N}_k + 1)$ rows enforce the continuity of the normal components of the electric flux density vector across the dielectric–free-space interfaces. The vector $\mathbf{A}$ contains the $N = \sum_{k=0}^{n} (N_k + 1)$ expansion coefficients of the free plus bound charge at the conductor peripheries, α_{lk}, and the vector $\hat{\mathbf{A}}$ contains the $\hat{N} = \sum_{k=0}^{n} (\hat{N}_k + 1)$ expansion coefficients of the bound charge at the dielectric– free-space peripheries, $\hat{\alpha}_{lk}$.

The entries in (3.87) can be obtained by considering a cylindrical boundary of radius r_b of infinite length shown in Fig. 3.24 which supports the charge distributions 1, $\cos(m\theta_b)$, $\sin(m\theta_b)$ around its periphery. This is identical to the

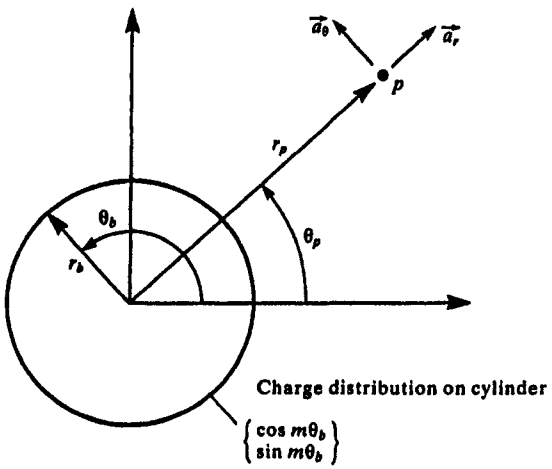

FIGURE 3.24 The general problem of determining the potential inside and outside a charge distribution.

problem of free charge around a conductor periphery considered in the previous section but here the charge distribution can represent free or bound charge distributions. Proceeding as in the previous section by modeling the charge distributions as weighted filaments of charge gives the potential both inside and outside the boundary. Similarly, the electric field due to these charge distributions can be obtained from the gradient of these potential solutions [A.1]:

$$\vec{E}(r_p, \theta_p) = -\nabla\phi = -\frac{\partial\phi}{\partial r}\,\hat{a}_r - \frac{\partial\phi}{\partial\theta}\,\hat{a}_\theta \tag{3.88}$$

Carrying out these operations, the potential and electric field at a point r_b, θ_b both *inside* and *outside* the charge distribution are given in Tables 3.2 and 3.3. Inverting equation (3.87) gives

$$\begin{bmatrix} \mathbf{A}_0 \\ \vdots \\ \mathbf{A}_i \\ \vdots \\ \mathbf{A}_N \\ \cdots \\ \hat{\mathbf{A}}_0 \\ \vdots \\ \hat{\mathbf{A}}_i \\ \vdots \\ \hat{\mathbf{A}}_{\hat{N}} \end{bmatrix} = \begin{bmatrix} \mathbf{B}_{00} & \cdots & \mathbf{B}_{0j} & \cdots & \mathbf{B}_{0N} \\ \vdots & \vdots & \vdots & \vdots & \vdots \\ \mathbf{B}_{i0} & \cdots & \mathbf{B}_{ij} & \cdots & \mathbf{B}_{iN} \\ \vdots & \vdots & \vdots & \vdots & \vdots \\ \mathbf{B}_{N0} & \cdots & \mathbf{B}_{Nj} & \cdots & \mathbf{B}_{NN} \\ \cdots & \cdots & \cdots & \cdots & \cdots \\ \hat{\mathbf{B}}_{00} & \cdots & \hat{\mathbf{B}}_{0j} & \cdots & \hat{\mathbf{B}}_{0N} \\ \vdots & \vdots & \vdots & \vdots & \vdots \\ \hat{\mathbf{B}}_{i0} & \cdots & \hat{\mathbf{B}}_{ij} & \cdots & \hat{\mathbf{B}}_{iN} \\ \vdots & \vdots & \vdots & \vdots & \vdots \\ \hat{\mathbf{B}}_{\hat{N}0} & \cdots & \hat{\mathbf{B}}_{\hat{N}j} & \cdots & \hat{\mathbf{B}}_{\hat{N}N} \end{bmatrix} \begin{bmatrix} \Phi_0 \\ \vdots \\ \Phi_j \\ \vdots \\ \Phi_N \\ \cdots \\ \mathbf{0} \\ \vdots \\ \mathbf{0} \\ \vdots \\ \mathbf{0} \end{bmatrix}$$

$$= \begin{bmatrix} \mathbf{B}_{00} & \cdots & \mathbf{B}_{0j} & \cdots & \mathbf{B}_{0N} \\ \vdots & \vdots & \vdots & \vdots & \vdots \\ \mathbf{B}_{i0} & \cdots & \mathbf{B}_{ij} & \cdots & \mathbf{B}_{iN} \\ \vdots & \vdots & \vdots & \vdots & \vdots \\ \mathbf{B}_{N0} & \cdots & \mathbf{B}_{Nj} & \cdots & \mathbf{B}_{NN} \\ \cdots & \cdots & \cdots & \cdots & \cdots \\ \hat{\mathbf{B}}_{i0} & \cdots & \hat{\mathbf{B}}_{0j} & \cdots & \hat{\mathbf{B}}_{0N} \\ \vdots & \vdots & \vdots & \vdots & \vdots \\ \hat{\mathbf{B}}_{i0} & \cdots & \hat{\mathbf{B}}_{ij} & \cdots & \hat{\mathbf{B}}_{iN} \\ \vdots & \vdots & \vdots & \vdots & \vdots \\ \hat{\mathbf{B}}_{\hat{N}0} & \cdots & \hat{\mathbf{B}}_{\hat{N}j} & \cdots & \hat{\mathbf{B}}_{\hat{N}N} \end{bmatrix} \begin{bmatrix} \Phi_0 \\ \vdots \\ \Phi_j \\ \vdots \\ \Phi_N \end{bmatrix} \tag{3.89}$$

TABLE 3.2 Matchpoint Outside the Charge Distribution, $r_p \geq r_b$

Charge distribution	Contribution to the potential at P	Contribution to the electric field at P
1	$-\dfrac{r_b \ln(r_p)}{\varepsilon}$	$\dfrac{r_b}{\varepsilon r_p}\hat{a}_r$
$\cos(m\theta_b)$	$\dfrac{r_b^{m+1}\cos(m\theta_p)}{2\varepsilon m r_p^m}$	$\dfrac{1}{2\varepsilon}\left(\dfrac{r_b}{r_p}\right)^{m+1}\begin{bmatrix}\cos(m\theta_p)\hat{a}_r \\ +\sin(m\theta_p)\hat{a}_\theta\end{bmatrix}$
$\sin(m\theta_b)$	$\dfrac{r_b^{m+1}\sin(m\theta_p)}{2\varepsilon m r_p^m}$	$\dfrac{1}{2\varepsilon}\left(\dfrac{r_b}{r_p}\right)^{m+1}\begin{bmatrix}\sin(m\theta_p)\hat{a}_r \\ -\cos(m\theta_p)\hat{a}_\theta\end{bmatrix}$

TABLE 3.3 Matchpoint Inside the Charge Distribution, $r_p < r_b$

Charge distribution	Contribution to the potential at P	Contribution to the electric field at P
1	$-\dfrac{r_b \ln(r_b)}{\varepsilon}$	0
$\cos(m\theta_b)$	$\dfrac{r_p^m \cos(m\theta_p)}{2\varepsilon m r_b^{m-1}}$	$-\dfrac{1}{2\varepsilon}\left(\dfrac{r_p}{r_b}\right)^{m-1}\begin{bmatrix}\cos(m\theta_p)\hat{a}_r \\ -\sin(m\theta_p)\hat{a}_\theta\end{bmatrix}$
$\sin(m\theta_b)$	$\dfrac{r_p^m \sin(m\theta_p)}{2\varepsilon m r_b^{m-1}}$	$-\dfrac{1}{2\varepsilon}\left(\dfrac{r_p}{r_b}\right)^{m-1}\begin{bmatrix}\sin(m\theta_p)\hat{a}_r \\ +\cos(m\theta_p)\hat{a}_\theta\end{bmatrix}$

Recall that the charge at the conductor–dielectric interface consists of *free charge plus bound charge*, $\rho_{lf} - \rho_{lb}$. The entries in the generalized capacitance matrix relate the *free charge* on the conductors to the conductor potentials. Therefore, according to (3.83) and (3.85) we must add the total (bound) charge at the dielectric–free-space surface to the total (bound plus free) charge at the conductor–dielectric surface in order to obtain the total free charge on the conductor. Thus, in a fashion similar to the bare conductor case above, the entries in the generalized capacitance matrix can be obtained from (3.89) as

$$\mathscr{C}_{ij} = \left.\frac{q_i}{\phi_j}\right|_{\phi_0 = \cdots = \phi_{j-1} = \phi_{j+1} = \cdots = \phi_n = 0} \tag{3.90}$$

$$= 2\pi r_{wi} \sum_{\text{first row}} \mathbf{B}_{ij} + 2\pi r_{wi} \sum_{\text{first row}} \hat{\mathbf{B}}_{ij}$$

where $\sum_{\text{first row}} \mathbf{B}_{ij}$ denotes the sum of the elements in the first row of the

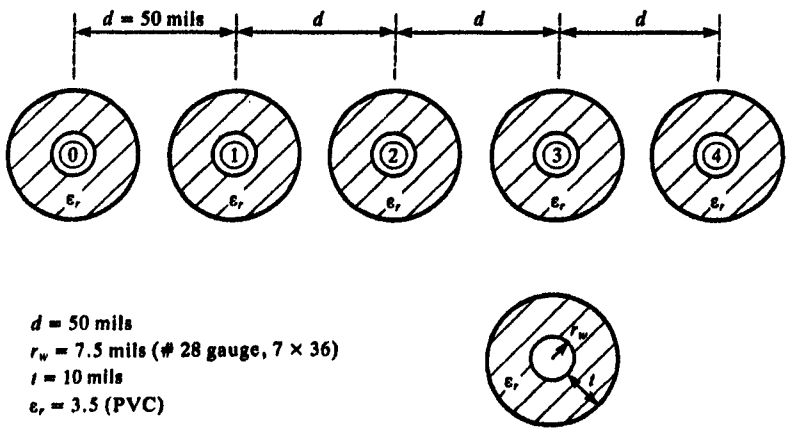

FIGURE 3.25 Dimensions of a five-wire ribbon cable for illustration of numerical results.

submatrix $\mathbf{B}_{ij}$ of (3.89) relating the α_{ik} coefficients of the bound plus free charge at the i-th conductor interface to the potential of the j-th conductor, ϕ_j, and $\sum_{\text{first row}} \hat{\mathbf{B}}_{ij}$ denotes the sum of the elements in the first row of the submatrix $\hat{\mathbf{B}}_{ij}$ of (3.89) relating the $\hat{\alpha}_{ik}$ coefficients of the bound charge at the dielectric–free-space interface for the i-th conductor to the potential of the j-th conductor, ϕ_j. Details of this are described in [C.1–C.7] and numerical results are also presented.

3.2.5 Computed Results: Ribbon Cables

As an illustration of numerical results for the results of the previous sections, consider the five-wire ribbon cable shown in Fig. 3.25. The center-to-center separations of the wires are 50 mils (1 mil = 0.001 inch). The wires are identical and are composed of #28 gauge (7 × 36) stranded wires with radii of $r_w = 7.5$ mils and polyvinyl chloride (PVC) insulations of thickness $t = 10$ mils and relative dielectric constant $\varepsilon_r = 3.5$. The generalized capacitance matrix was computed using the method of the previous section and ten Fourier coefficients around each wire surface (the constant term and nine cosine terms) and ten Fourier coefficients around each dielectric–free-space surface. The results are computed using the **RIBBON.FOR** computer program described in Appendix A which implements the method described in the previous section and are given in Table 3.4. The results computed using twenty Fourier coefficients around the wire and dielectric surfaces are virtually identical to those using ten coefficients indicating convergence of the solution. Alternatively, the results may be calculated with the **GETCAP** program described in [C.2, C.6, C.7]. We have shown only the upper diagonal terms since, because of symmetry, the generalized capacitance matrix is symmetric. Choosing one of the outermost conductors as the reference conductor, the transmission-line-capacitance matrix is

TABLE 3.4 Generalized Capacitances for the Five-Wire Ribbon Cable With and Without the Insulation Dielectric

Entry	With dielectric (pF/m)	Without dielectric (pF/m)
$\mathscr{C}_{00}$	26.775 8	18.223 2
$\mathscr{C}_{01}$	−17.497 9	−9.968 57
$\mathscr{C}_{02}$	−2.899 39	−2.575 14
$\mathscr{C}_{03}$	−1.671 39	−1.555 14
$\mathscr{C}_{04}$	−2.136 72	−1.780 84
$\mathscr{C}_{11}$	38.325 6	23.549 2
$\mathscr{C}_{12}$	−15.817 7	−8.722 27
$\mathscr{C}_{13}$	−2.109 30	−1.986 98
$\mathscr{C}_{14}$	−1.671 38	−1.555 14
$\mathscr{C}_{22}$	38.541 2	23.780 2
$\mathscr{C}_{23}$	−15.817 7	−8.722 27
$\mathscr{C}_{24}$	−2.899 41	−2.575 14
$\mathscr{C}_{33}$	38.325 5	23.549 2
$\mathscr{C}_{34}$	−17.497 8	−9.968 58
$\mathscr{C}_{44}$	26.775 8	18.223 2

TABLE 3.5 The Transmission-Line Capacitances for the Five-Wire Ribbon Cable With and Without the Insulation Dielectrics

Entry	With dielectric (pF/m)	Without dielectric (pF/m)	Effective dielectric constant, ε'_r
C_{11}	38.152	23.345	1.634
C_{12}	−15.974	−8.9057	1.794
C_{13}	−2.2829	−2.1907	1.042
C_{14}	−2.0343	−1.9178	1.061
C_{22}	38.401	23.615	1.626
C_{23}	−15.974	−8.9057	1.794
C_{24}	−3.2263	−2.9018	1.112
C_{33}	38.152	23.345	1.634
C_{34}	−17.861	−10.331	1.729
C_{44}	26.017	17.577	1.480

given in Table 3.5. Once again, only the upper diagonal elements are shown because of the symmetry of **C**. The rightmost column shows the *effective dielectric constant* which is the ratio of the per-unit-length capacitances with and without the dielectric.

TABLE 3.6 The Transmission-Line Inductances for the Five-Wire Ribbon Cable Computed Exactly and Using the Wide-Separation Approximations

Entry	Exact (μH/m)	Wide separation approx (μH/m)	Percent error
L_{11}	0.748 34	0.758 85	1.40
L_{12}	0.507 11	0.518 05	2.16
L_{13}	0.455 27	0.460 52	1.15
L_{14}	0.432 95	0.436 96	0.93
L_{22}	1.013 2	1.036 1	2.26
L_{23}	0.719 84	0.737 78	2.49
L_{24}	0.645 69	0.656 68	1.70
L_{33}	1.173 8	1.198 3	2.09
L_{34}	0.858 42	0.876 41	2.10
L_{44}	1.291 4	1.313 4	1.71

The per-unit-length inductance matrix, **L**, can be computed from the inverse of the capacitance matrix *with the dielectric insulations removed*, $\mathbf{C}_o$, as $\mathbf{L} = \mu_o \varepsilon_o \mathbf{C}_o^{-1}$. Using the above computed results we obtain Table 3.6. The wide-separation approximations were computed from (3.63) using the FORTRAN program **WIDESEP.FOR** described in Appendix A as

$$l_{11} = \frac{\mu_o}{\pi} \ln\left(\frac{d}{r_w}\right)$$

$$l_{22} = \frac{\mu_o}{\pi} \ln\left(\frac{2d}{r_w}\right)$$

$$l_{33} = \frac{\mu_o}{\pi} \ln\left(\frac{3d}{r_w}\right)$$

$$l_{44} = \frac{\mu_o}{\pi} \ln\left(\frac{4d}{r_w}\right)$$

$$l_{12} = \frac{\mu_o}{2\pi} \ln\left(\frac{2d}{r_w}\right)$$

$$l_{13} = \frac{\mu_o}{2\pi} \ln\left(\frac{3}{2}\frac{d}{r_w}\right)$$

$$l_{14} = \frac{\mu_o}{2\pi} \ln\left(\frac{4}{3}\frac{d}{r_w}\right)$$

TABLE 3.7 The Generalized Capacitances for the Three-Wire Ribbon Cable With and Without the Dielectric Insulations

Entry	With dielectric (pF/m)	Without dielectric (pF/m)
$\mathscr{C}_{00}$	26.2148	17.6900
$\mathscr{C}_{01}$	−18.0249	−10.5205
$\mathscr{C}_{02}$	−5.033 25	−4.225 44
$\mathscr{C}_{11}$	37.8189	22.9694
$\mathscr{C}_{12}$	−18.0249	−10.5205
$\mathscr{C}_{22}$	26.2148	17.6901

$$l_{23} = \frac{\mu_o}{2\pi} \ln\left(\frac{6d}{r_w}\right)$$

$$l_{24} = \frac{\mu_o}{2\pi} \ln\left(\frac{4d}{r_w}\right)$$

$$l_{34} = \frac{\mu_o}{2\pi} \ln\left(\frac{12d}{r_w}\right)$$

Observe that the wide-separation approximations are within some 2% of the exact results even though the ratio of adjacent wire spacing to wire radius is $d/r_w = 6.67$. Consequently, the entries in the inductance matrix can be reliably computed with this less computationally expensive method.

In order to gauge the effect of neighboring wires on these results and to obtain the capacitance and inductance matrices to be used in a later example, consider a *three-wire ribbon cable.* The wire separations, radii, insulation thicknesses and type are identical to the five-wire case. The exact generalized capacitance matrix is again computed with the **RIBBON.FOR** computer program described in Appendix A and the entries are given in Table 3.7. The per-unit-length transmission-line-capacitance matrices, $\mathbf{C}$ and $\mathbf{C}_0$, are given in Table 3.8. The per-unit-length inductances computed exactly as $\mathbf{L} = \mu_0 \varepsilon_0 \mathbf{C}_0^{-1}$ and using the wide-separation approximations are given in Table 3.9. The wide-separation approximations are again computed from (3.63) as

$$l_{11} = \frac{\mu_o}{\pi} \ln\left(\frac{d}{r_w}\right)$$

$$l_{12} = \frac{\mu_o}{2\pi} \ln\left(\frac{2d}{r_w}\right)$$

$$l_{22} = \frac{\mu_o}{\pi} \ln\left(\frac{2d}{r_w}\right)$$

TABLE 3.8 The Transmission-Line Capacitances for the Three-Wire Ribbon Cable With and Without the Insulation Dielectrics

Entry	With dielectric (pF/m)	Without dielectric (pF/m)	Effective dielectric constant, ε_r'
C_{11}	37.432	22.494	1.664
C_{12}	−18.716	−11.247	1.664
C_{22}	24.982	16.581	1.507

TABLE 3.9 The Transmission-Line Inductances for the Three-Wire Ribbon Cable Computed Exactly and Using the Wide-Separation Approximations

Entry	Exact (μH/m)	Wide separation approx (μH/m)	Percent error
L_{11}	0.748 50	0.758 85	1.38
L_{12}	0.507 70	0.518 05	2.04
L_{22}	1.015 4	1.036 1	2.04

Once again, the wide-separation approximations give results for the entries in the per-unit-length inductance matrix that are within some 2% of the exact values computed from $\mathbf{L} = \mu_0 \varepsilon_0 \mathbf{C}_0^{-1}$.

Figure 3.26 illustrates the convergence of the method for the three-wire ribbon cable. The per-unit-length inductances and per-unit-length capacitances are plotted vs. the number of Fourier coefficients around the wire and dielectric boundaries in Fig. 3.26(a) and 3.26(b), respectively. Observe that the inductances converge to accurate values for only two Fourier coefficients, whereas the capacitances require of the order of three or four Fourier coefficients for convergence.

3.3 MULTICONDUCTOR LINES HAVING CONDUCTORS OF RECTANGULAR CROSS SECTION

Determining the entries in the per-unit-length parameter matrices **L**, **C**, and **G** for conductors of rectangular cross section is the same as for conductors of circular cross section (wires)—the solution of Laplace's or Poisson's equation in the two-dimensional transverse plane, e.g.,

$$\nabla^2 \phi(x, y) = \frac{\partial^2 \phi}{\partial x^2} + \frac{\partial^2 \phi}{\partial y^2} = \rho(x, y) \tag{3.91}$$

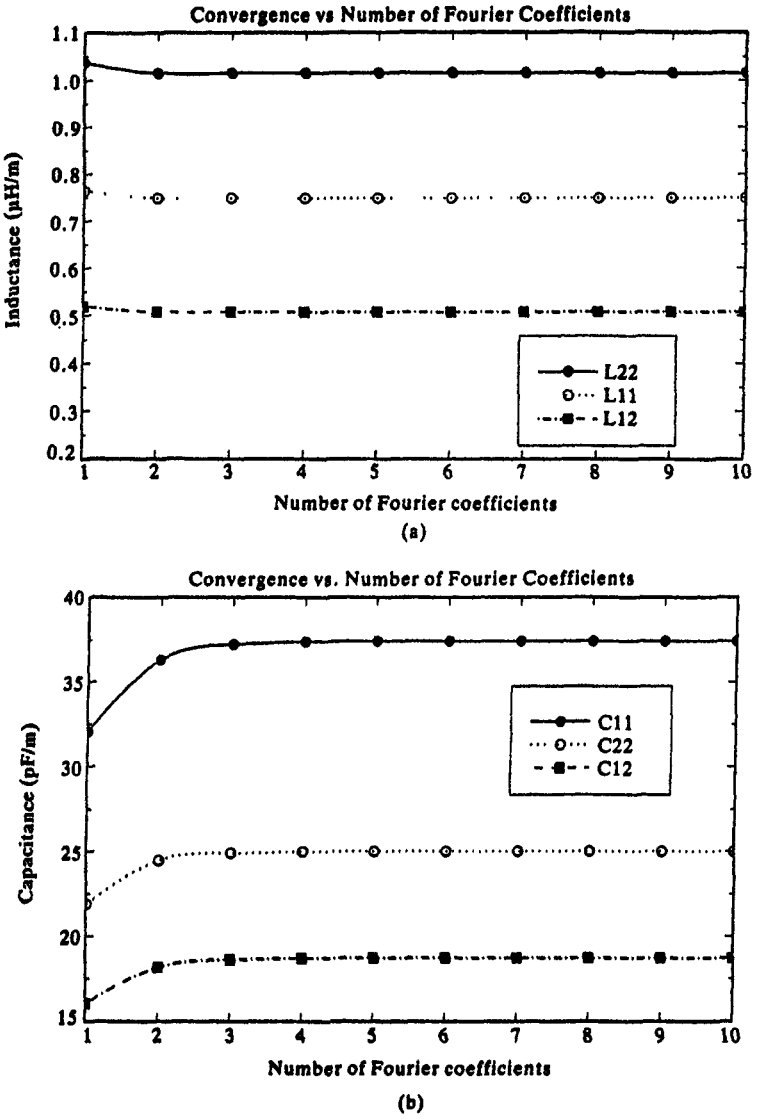

FIGURE 3.26 Convergence of the per-unit length parameters of the five-wire ribbon cable versus number of Fourier expansion coefficients: (a) inductances, (b) capacitances.

There are various methods for solving this equation. Unless the problem boundaries fit some coordinate system, the usual solution methods determine an approximate solution using various numerical techniques that we will discuss in this section.

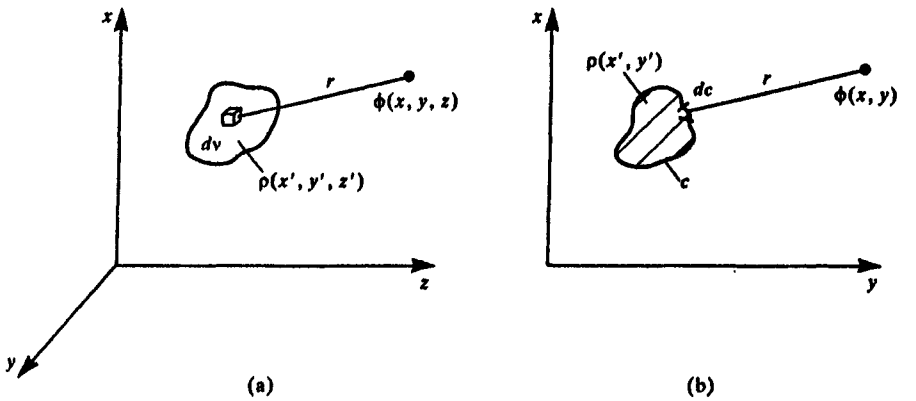

FIGURE 3.27 Illustrations of the solution of Poisson's equation: (a) in three dimensions and (b) in two dimensions.

3.3.1 Method of Moments (MOM) Techniques

Method of moments (MOM) techniques essentially solve integral equations where the unknown is in the integrand. An example is the integral form of Poisson's equation [A.1]:

$$\phi(x, y, z) = \frac{1}{4\pi\varepsilon} \iiint_v \frac{\rho(x', y', z')}{r}\, dv \tag{3.92}$$

where a charge distribution ρ is distributed throughout some volume v as illustrated in Fig. 3.27(a). Ordinarily we know or prescribe the potential at points in the region (for example, on perfectly conducting bodies) and wish to find the charge distribution that produces it. Thus we need to solve an integral equation for the integrand [A.1, 4–7].

The problems of interest here are perfect conductors and/or dielectric bodies in the two-dimensional plane which are infinite in length (in the z direction) and have some unknown surface charge density, $\rho(x, y)$ C/m^2, per unit of length in the z direction residing on their surfaces as illustrated in Fig. 3.27(b). In this case, the integral form of Poisson's equation in (3.92) cannot be used to determine the potential distribution of this infinite length charge distribution since the structure extends to infinity in the z direction and we must find alternate methods. A very common way of doing this is to approximate the charge distribution around the two-dimensional conductor periphery as filaments of charge and use the basic problem of the potential of an infinitesimal line charge that was developed in Section 3.2.1.2. This forms the basis for numerical techniques that are used to analyze these two-dimensional structures of infinite length for determining the per-unit-length parameters [4–7]. Thus

we initially solve the problem of the potential of an infinitely long filament of charge carrying a per-unit-length charge (per unit length in the z direction in C/m^2) which is uniformly distributed in the z direction. The potential at a point is the sum of the potentials of each line charge that makes up the desired charge distribution around the conductor periphery. The potential in this case is only meaningful with respect to the potential of a reference point in the two-dimensional plane because the structure is infinite in length in the z direction. Again, as for the case of ribbon cables, it can be readily shown that we may omit the reference point and its potential so long as the system under consideration is charge neutral [C.5, C.6].

In order to illustrate the general method, consider a system of $(n + 1)$ perfect conductors each having a prescribed potential ϕ_i with $i = 0, 1, \ldots, n$. In order to determine the potential distribution in the two-dimensional plane, we represent the per-unit-length charge distribution over the i-th conductor as a linear combination of N_i *basis functions* as in the case of ribbon cables considered earlier:

$$\rho_i = \alpha_{i1}\rho_{i1} + \alpha_{i2}\rho_{i2} + \alpha_{i3}\rho_{i3} + \cdots = \sum_{k=1}^{N_i} \alpha_{ik}\rho_{ik} \tag{3.93}$$

The ρ_{ik} basis functions will be prescribed and the unknown coefficients α_{ik} are to be determined to satisfy the boundary condition that the potential over the i-th conductor is ϕ_i. The potential at a point due to this representation will be a linear combination of the charge expansion functions as

$$\phi(x, y) = \sum_{k=1}^{N_i} K_{ik}\alpha_{ik} \tag{3.94}$$

Each coefficient, K_{ik}, is determined as the contribution to the potential due to each basis function alone:

$$K_{ik} = \phi|_{\alpha_{ik}=1, \alpha_{i1}, \ldots, \alpha_{ik-1}, \alpha_{ik+1}, \ldots, \alpha_{iN_i}=0} \tag{3.95}$$

As in the case of a ribbon cable considered previously, there are many possible forms for the expansion or basis functions, ρ_{ik}. *Entire domain expansions* seek to represent the charge distribution over the conductor surface as functions each of which are nonzero over the entire contour of the surface in the same manner as a Fourier series represents a time-domain function using basis functions defined over the time interval encompassing one complete period. This was the technique used earlier to expand the charge distributions around the wire and dielectric insulation peripheries of ribbon cables. *Subdomain expansions* seek to represent the charge distribution over discrete segments of the contour [C.1, C.3]. Each of the expansion basis functions, ρ_{ik}, is defined over the discrete segments of the contour, c_{ik}, and is zero over the other segments. We will concentrate on the subdomain expansion method. There are many ways

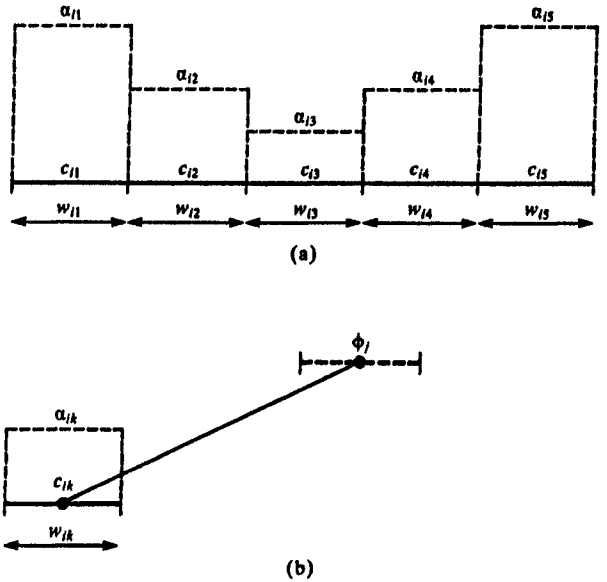

FIGURE 3.28 Illustration of the pulse expansion of a charge distribution on a flat strip.

of choosing the expansion functions over the segments. One of the simplest ways is to represent the charge distribution as a "staircase function" where the charge distribution is constant over the segments of the contour:

$$\rho_{ik} = \begin{cases} 1 \in c_{ik} \\ 0 \notin c_{ik} \end{cases} \tag{3.96}$$

This is referred to as the *pulse expansion method* and the charge distribution is assumed constant over the segments c_{ik}. Figure 3.28(a) illustrates this approximation of a charge distribution over the surface of an infinitesimally thin, perfectly conducting plate that extends to infinity in the z direction. Thus the charge distribution we are representing has variation in the x, y plane and is uniformly distributed in the z direction. The units of this charge distribution are therefore C/m^2.

Once the expansion functions are chosen we need to generate a set of linearly independent equations in terms of the expansion coefficients, α_{ik}, which can be solved for them thus generating via (3.94) an approximation to the charge distribution over that surface. The total charge (per unit length) in the z direction) in C/m is obtained by summing the charges of the subsections of that conductor:

$$q_i = \sum_{k=1}^{N_i} \alpha_{ik} \int_{c_i} \rho_{ik}\, dc \tag{3.97}$$

In the case of the pulse expansion method, this simplifies to

$$q_i = \sum_{k=1}^{N_i} \alpha_{ik} w_{ik} \tag{3.98}$$

where w_{ik} is the width of the k-th segment of the i-th conductor. From these results we can compute the per-unit-length capacitances. There are many ways of generating the required equations. One rather simple method is the method of *point matching*. For illustration consider a system of $(n + 1)$ conductors each having a prescribed potential of ϕ_i for $i = 0, \ldots, n$. We next enforce the potential of each conductor, ϕ_i, due to all charge distributions in the system to be the potential of that conductor at the center of the subsection of the conductor. This is illustrated for the pulse expansion method in Fig. 3.28(b). A typical resulting equation is of the form

$$\phi_i = \sum_{k=1}^{N_0} K_{0k}\alpha_{0k} + \cdots + \sum_{k=1}^{N_i} K_{ik}\alpha_{ik} + \cdots + \sum_{k=1}^{N_n} K_{nk}\alpha_{nk} \tag{3.99}$$

Choosing a total of

$$N = \sum_{k=0}^{n} N_k \tag{3.100}$$

points on the conductors gives the following set of N equations in terms of the expansion coefficients:

$$\Phi = \mathbf{D}\mathbf{A} \tag{3.101a}$$

or, in expanded form,

$$\begin{bmatrix} \Phi_0 \\ \vdots \\ \Phi_i \\ \vdots \\ \Phi_n \end{bmatrix} = \begin{bmatrix} \mathbf{D}_{00} & \cdots & \mathbf{D}_{0j} & \cdots & \mathbf{D}_{0n} \\ \vdots & \vdots & \vdots & \vdots & \vdots \\ \mathbf{D}_{i0} & \cdots & \mathbf{D}_{ij} & \cdots & \mathbf{D}_{in} \\ \vdots & \vdots & \vdots & \vdots & \vdots \\ \mathbf{D}_{n0} & \cdots & \mathbf{D}_{nj} & \cdots & \mathbf{D}_{nn} \end{bmatrix} \begin{bmatrix} \mathbf{A}_0 \\ \vdots \\ \mathbf{A}_j \\ \vdots \\ \mathbf{A}_n \end{bmatrix} \tag{3.101b}$$

The vector of potentials at the matchpoints on the i-th conductor is denoted as

$$\Phi_i = \begin{bmatrix} \phi_i \\ \vdots \\ \phi_i \\ \vdots \\ \phi_i \end{bmatrix} \tag{3.101c}$$

and the vector of expansion coefficients of the charge distribution on the i-th conductor is denoted as

$$\mathbf{A}_i = \begin{bmatrix} \alpha_{i1} \\ \vdots \\ \alpha_{ik} \\ \vdots \\ \alpha_{iN_i} \end{bmatrix} \tag{3.101d}$$

Inverting (3.101b) gives

$$\mathbf{A} = \mathbf{D}^{-1}\Phi \tag{3.102a}$$

or, in expanded form,

$$\begin{bmatrix} \mathbf{A}_0 \\ \vdots \\ \mathbf{A}_i \\ \vdots \\ \mathbf{A}_n \end{bmatrix} = \begin{bmatrix} \mathbf{B}_{00} & \cdots & \mathbf{B}_{0j} & \cdots & \mathbf{B}_{0n} \\ \vdots & \vdots & \vdots & \vdots & \vdots \\ \mathbf{B}_{i0} & \cdots & \mathbf{B}_{ij} & \cdots & \mathbf{B}_{in} \\ \vdots & \vdots & \vdots & \vdots & \vdots \\ \mathbf{B}_{n0} & \cdots & \mathbf{B}_{nj} & \cdots & \mathbf{B}_{nn} \end{bmatrix} \begin{bmatrix} \Phi_0 \\ \vdots \\ \Phi_j \\ \vdots \\ \Phi_n \end{bmatrix} \tag{3.102b}$$

Once the expansion coefficients are obtained from (3.102), the total charge (per unit of length in the z direction in C/m) can be obtained from (3.97). The *generalized capacitance matrix*, $\mathscr{C}$, described in Section 3.1.4 can then be obtained. In the case of point matching and pulse expansion functions, as with flat conductors, the entries in the generalized capacitance matrix can be directly obtained from (3.102) as

$$\mathscr{C}_{ij} = w_{i1} \sum_{\text{row } 1} \mathbf{B}_{ij} + w_{i2} \sum_{\text{row } 2} \mathbf{B}_{ij} + \cdots + w_{iN_i} \sum_{\text{row } N_i} \mathbf{B}_{ij} \tag{3.103a}$$

where w_{ik} is the width of the k-th subsection of the i-th conductor. If the widths of all the conductor segments are chosen to be w, then the elements of the generalized capacitance matrix simplify to

$$\mathscr{C}_{ij} = w \sum \mathbf{B}_{ij} \tag{3.103b}$$

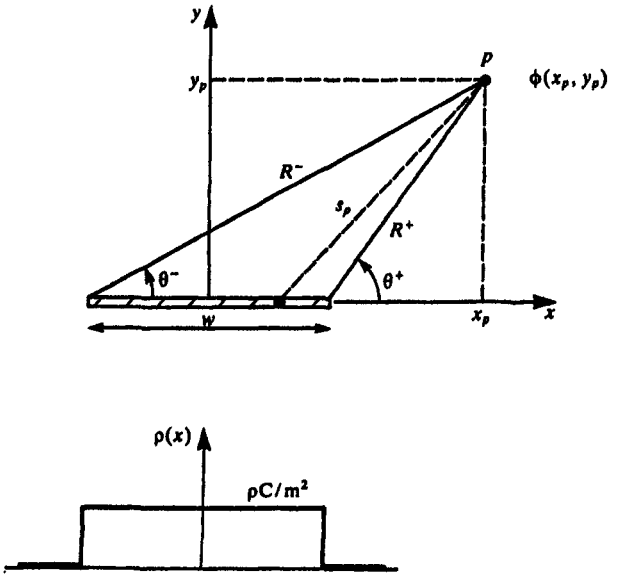

FIGURE 3.29 Calculation of the potential due to a constant charge distribution on a flat strip.

These simple results are due to the fact that a submatrix of (3.102b) is

$$\begin{bmatrix} \alpha_{i1} \\ \vdots \\ \alpha_{ik} \\ \vdots \\ \alpha_{iN_i} \end{bmatrix} = [\mathbf{B}_{ij}] \begin{bmatrix} \phi_j \\ \vdots \\ \phi_j \\ \vdots \\ \phi_j \end{bmatrix} \tag{3.104a}$$

or, in expanded form,

$$\alpha_{ik} = \left\{ \sum_{\text{row } k} \mathbf{B}_{ij} \right\} \phi_j \tag{3.104b}$$

Thus the basic subproblem is the integration in (3.95). In order to illustrate this, consider the infinitesimally thin conducting strip of width w and infinite length supporting a charge distribution ρ C/m^2 that is constant along the strip cross section as shown in Fig. 3.29. If we treat this as an array of wire filaments each of which bears a charge per unit of filament length of $\rho\, dx$ C/m, then we may determine the potential at a point as the sum of the potentials of these filaments again using the basic result for the potential of a filament given in

(3.30) or (3.71) [4, 7]:

$$\phi(w, x_p, y_p) = -\frac{\rho}{2\pi\varepsilon}\int_{-w/2}^{w/2} \ln[\sqrt{(x_p - x)^2 + (y_p)^2}]\, dx \tag{3.105}$$

$$= -\frac{\rho}{4\pi\varepsilon}\left\{\left(x_p + \frac{w}{2}\right)\ln\left[\left(x_p + \frac{w}{2}\right)^2 + y_p^2\right]\right.$$

$$-\left(x_p - \frac{w}{2}\right)\ln\left[\left(x_p - \frac{w}{2}\right)^2 + y_p^2\right] - 2w$$

$$\left. + 2y_p\left[\tan^{-1}\left(\frac{x_p + \frac{w}{2}}{y_p}\right) - \tan^{1}\left(\frac{x_p - \frac{w}{2}}{y_p}\right)\right]\right\}$$

These integrals are evaluated using [8]. This may be simplified somewhat if we denote the distances from the edges of the strip as R^+ and R^- and the angles as θ^+ and θ^- as shown in Fig. 3.29. In terms of these (3.105) becomes

$$\phi(w, x_p, y_p) = \frac{\rho}{2\pi\varepsilon}\left[x_p \ln\left(\frac{R^+}{R^-}\right) - \frac{w}{2}\ln(R^+R^-) + w - y_p(\theta^+ - \theta^-)\right] \tag{3.106}$$

In the case where the field or observation point lies at the midpoint of the strip in question, the integral in (3.105) is singular but integrable. The result is [8]

$$\phi(w) = \frac{\rho}{2\pi\varepsilon} w\left[1 - \ln\left(\frac{w}{2}\right)\right] \tag{3.107}$$

The electric field due to this charge distribution will be needed for problems that involve dielectric interfaces. The electric field can be computed from this result as

$$\vec{E} = -\frac{\partial\phi}{\partial x}\hat{a}_x - \frac{\partial\phi}{\partial y}\hat{a}_y \tag{3.108}$$

where

$$E_x = \frac{\rho}{2\pi\varepsilon}\ln\left(\frac{R^+}{R^-}\right) \tag{3.109a}$$

$$E_y = -\frac{\rho}{2\pi\varepsilon}[\theta^+ - \theta^-] \tag{3.109b}$$

As an illustration of this method consider the rectangular conducting box shown in Fig. 3.30. The four walls are insulated from one another and are maintained at potentials of $\phi_1 = 0$, $\phi_2 = 10\text{V}$, $\phi_3 = 20\text{V}$, $\phi_4 = 30\text{V}$. Suppose

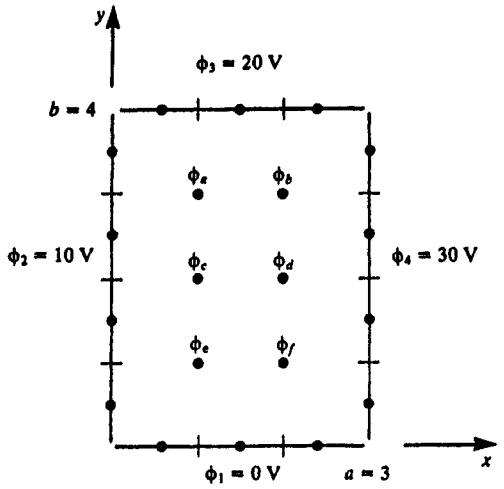

FIGURE 3.30 A two-dimensional problem for demonstration of the solution of Laplace's equation via the pulse expansion–point matching method.

TABLE 3.10 Comparison of MOM and Exact Results for the Potential in Fig. 3.30

	MOM	Exact
$\phi_a(x = 1, y = 3)$	16.433	16.478 4
$\phi_b(x = 2, y = 3)$	21.834	21.849 9
$\phi_c(x = 1, y = 2)$	14.130	14.157 5
$\phi_d(x = 2, y = 2)$	20.514	20.492 4
$\phi_e(x = 1, y = 1)$	9.527	9.609 42
$\phi_f(x = 2, y = 1)$	14.934	14.981 0

we divide the two vertical conductors into four segments each and the horizontal members into three segments each. Using pulse expansion functions for each segment and point matching gives fourteen equations in fourteen unknowns (the levels of the assumed constant charge distributions over each segment). Using the above results Table 3.10 gives the potentials at the six interior points. The *exact* results were obtained via a direct solution of Laplace's equation using separation of variables. In terms of the general parameters denoted in Fig. 3.30, the solution is [9]

$$\phi(x, y) = \sum_{\substack{n=1 \\ n\text{odd}}}^{\infty} \left\{ \frac{\alpha}{n\pi} \frac{\sin(n\pi y/b)}{\sinh(n\pi a/b)} \left[\phi_4 \sinh\left(\frac{n\pi x}{b}\right) + \phi_2 \sinh\left(\frac{n\pi}{b}(a - x)\right) \right] \right.$$
$$\left. + \frac{4}{n\pi} \frac{\sin(n\pi x/a)}{\sinh(n\pi a/b)} \left[\phi_3 \sinh\left(\frac{n\pi y}{a}\right) + \phi_1 \sinh\left(\frac{n\pi}{a}(b - y)\right) \right] \right\}$$

where $a = 3$, $b = 4$, and $\phi_1 = 0$, $\phi_2 = 10\text{V}$, $\phi_3 = 20\text{V}$, $\phi_4 = 30\text{V}$. The solution using finite difference and finite element methods will be given in a subsequent subsection.

This method can be readily extended to systems that contain dielectric bodies as in the case of printed circuit boards by similarly expanding the bound charge on those surfaces as above. The solution technique follows that for the ribbon cable.

The pulse expansion–point matching technique described above is particularly simple to implement in a digital computer program. Achieving convergence generally requires a rather large computational expense since the conductor subsections must be chosen sufficiently small to give an accurate representation of the charge distributions. This is particularly true in the case of lands on PCB's where the charge distribution peaks at the edges of each land. There are other choices of expansion functions such as triangles or piecewise sinusoidal functions but the programming complexity also increases. Another way of improving convergence is to use another method of generating the required number of equations other than point matching. A reasonably simple but effective method is the Galerkin method. This is closely related to the Rayleigh–Ritz variational method of minimizing a functional [6]. Although the following explanation overlooks some of the finer points of the method, it illustrates the computational details. Consider Fig. 3.31(a) showing contours

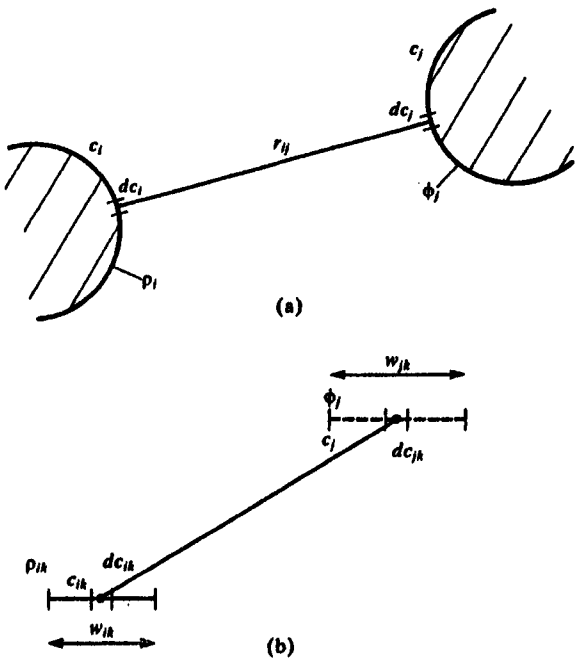

FIGURE 3.31 Illustration of the general determination of potential via the Galerkin method.

on the i-th and j-th conductors of the system which is infinite in extent in the z direction. The potential at some point on the j-th conductor due to the charge expansion basis functions of the i-th conductor is a function of the distance r_{ij} between the differential segments of each conductor:

$$\phi_j(r_{ij}) = \sum_{k=1}^{N_i} K_{ik}(r_{ij})\alpha_{ik} \tag{3.110}$$

Multiply this by the m-th basis function of the charge expansion of the j-th conductor and integrate over c_j:

$$\int_{c_j} \rho_{jm}\phi_j(r_{ij})\, dc_j = \sum_{k=1}^{N_i} \alpha_{ik}\left[\int_{c_j} \rho_{jm}K_{ik}(r_{ij})\, dc_j\right] \tag{3.111}$$

Likewise add in the contributions from the charge distributions of the other conductors to this equation to give

$$\int_{c_j} \rho_{jm}\phi_j(r)\, dc_j = \sum_{i=0}^{N}\sum_{k=1}^{N_i} K'_{ik}\alpha_{ik} \tag{3.112}$$

This method amounts to "weighting" the potential over the conductor rather than matching it at discrete points on the conductor. If pulse expansion functions are used, the method averages the potential over the conductor. Repeating this for the other expansion functions and all conductors gives the required number of equations to be solved for the charge expansion coefficients. In the case of pulse expansion functions and flat conductor segments of width w_{ik}, this simplifies to

$$w_{jk}\phi_j = \sum_{i=0}^{N}\sum_{k=1}^{N_i} K'_{ik}\alpha_{ik} \tag{3.113}$$

Thus the form of the equations in (3.101b) is the same but the entries in $\mathbf{D}$ are changed and the entries in Φ are multiplied by the segment widths, w_{jk}.

It is particularly interesting to observe that *the wide-separation approximations developed for widely spaced wires in Section* 3.2.3 *can be shown to be equivalent to using the Galerkin method when only one expansion function (the constant one) is used for the charge distribution about each wire.* This observation gives added credence to those seemingly crude approximations.

3.3.1.1 Applications to Printed Circuit Boards The above MOM method can be adapted to the computation of the per-unit-length capacitances of conductors with rectangular cross sections as occur on printed circuit boards (PCB's). Consider a typical PCB shown in Fig. 3.32(a) having infinitesimally thin conducting lands on the surface of a dielectric board of thickness t and relative dielectric constant of ε_r. The widths of the lands are denoted as w_i and the